Supporting Information

Designing vehicle-free anti-bacterial topical hydrogel from Fmoc-diphenylalanine.

Nabanita Roy[a], Hemanta Kumar Datta[a], Rajdip Roy[a] and Parthasarathi Dastidar[a]*

[a]School of Chemical Sciences, Indian Association for the Cultivation of Science (IACS), 2A and 2B, Raja S. C. Mullick Road, Jadavpur, Kolkata - 700032, West Bengal, India

*e-mail: ocpd@iacs.res.in

Contents

Experimental Section

Materials: All the chemicals were commercially bought and used without any further purification. All the solvents were of laboratory reagent grade and used without any distillation. 3-(4,5-Dimethyl-2-thiazolyl)-2,5-diphenyl-2H-tetrazolium bromide (MTT), and Resazurin (7-Hydroxy-3H-phenoxazin-3-one 10-oxide) was bought from Sigma-Aldrich Chemical Company. *Escherichia coli* (MTCC 1687), *Staphylococcus aureus* (MTCC 96) and *Pseudomonas aeruginosa* (MTCC 1688) was obtained from Microbial Type Culture Collection and Gene Bank (MTCC), India. HEK 293 cell line was bought from NCCS Pune, India.

Methods: FTIR spectra were recorded by a PerkinElmer FTIR spectrometer (spectrometer two) instrument. Both ^{1}H and ^{13}C NMR spectra were recorded with 400 and 500 MHz spectrometers (Bruker Ultrashield Plus-500). TEM images were captured with JEOL JEM 2100F (for field emission gun-TEM) and JEOL JEM 2010/11 [for high-resolution TEM (HR-TEM)] instruments using 300 mesh carbon-coated copper TEM grids. SEM images were collected in JEOL JSM-7500F field emission scanning electron microscope. Rheology studies were carried out with the Anton Paar Modular Compact Rheometer MCR 102. PXRD data was recorded using Rigaku Smartlab (40 kV, 110 mA) equipped with a 0D detector (HyPix-3000) (Cu Kα1 radiation, λ = 1.5406 Å, scan speed = 50°/min, step size = 0.010°). Two different diffractometers (Bruker APEX III D8 Venture, PHOTON II detector, Mo Kα, λ = 0.7107 and Bruker APEX II, CCD area detector, Mo K*α*, λ= 0.7107 Å) was used for SXRD data collection. Bacteria were cultured in nutrient broth or in nutrient agar media (1% agar) at 37 °C in a Bio-Oxygen Demand (BOD) shaker incubator. MTT assays were conducted by using a multi-plate ELISA reader (Varioskan Flash Elisa Reader, Thermo Fisher).

Synthesis of dipeptides BocFF and FmocFF : The corresponding *N*-protected-L-phenylalanine (**BocF or FmocF**) (5 mmoles,) and *N*-hydroxysuccinamide were dissolved in dry THF (100 mL) in a 250 mL round-bottom flask. Dicyclohexylcarbodiimide (DCC) in dry THF (50 mL) (7.5 mmoles,) was taken and added dropwise into this solution under inert conditions, and the reaction mixture was stirred for 12 hrs. The precipitate obtained was filtered. L-phenylalanine (5 mmoles,) dissolved in aqueous Na_2CO_3 (20 mL) (4.5 mmoles) was then added in the filtrate and was kept under stirring condition for 36 hrs (approx.). The final solution was further filtered to remove excess precipitate from the second step. The filtrate thus obtained was evaporated in rotary evaporator to remove THF and the dipeptide was recovered upon acidification with 1(N) HCl solution. The white precipitate was filtered, dried under vacuum, and purified with the help of column chromatography using MeOH in DCM. The final product **BocFF** or **FmocFF** was isolated and characterized (Scheme S1).

Synthesis of PAM salts: The organic salts were prepared by reacting equimolar quantities of the acids, i.e, commercially bought *N*-protected amino acids (**BocF** and **FmocF**) and the synthesized *N*-protected dipeptides (**BocFF** and **FmocFF**), with the amines in methanol at room temperature. The resultant solution (1:1 mixture of acid and amine) was dried in a rotary evaporator and isolated as solid compound with near-quantitative yield (Scheme S2). The complete salt formation was characterized by FT-IR spectra where a shift in stretching frequency of COOH (for acids) to COO^- (for salts) was observed.

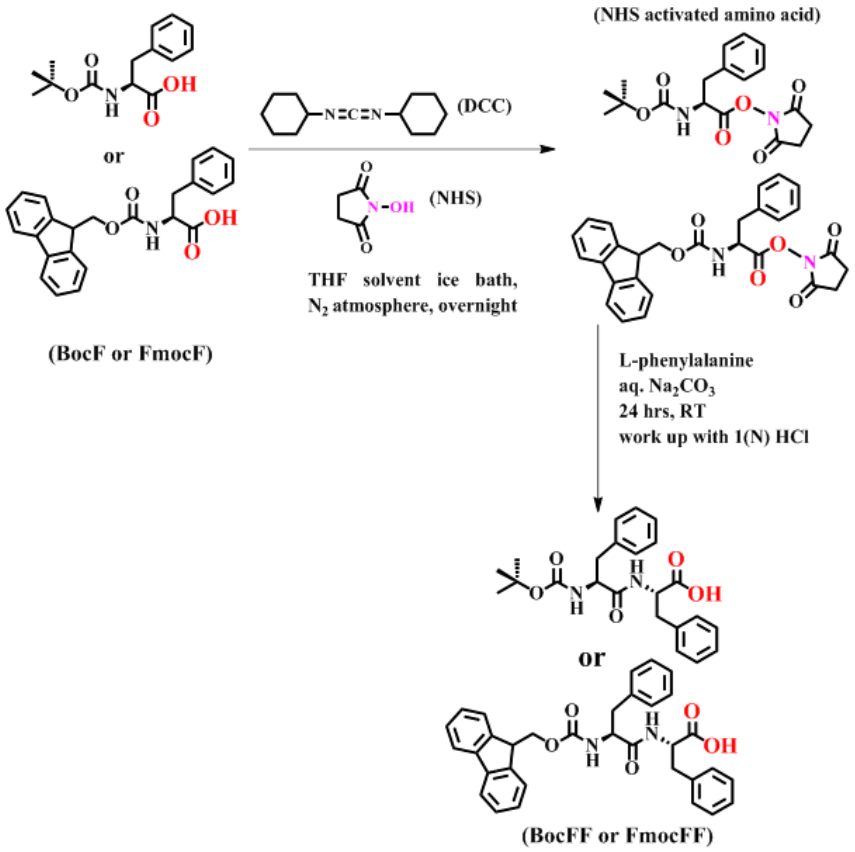

Scheme S1: Synthetic strategy for dipeptides **BocFF** and **FmocFF.**

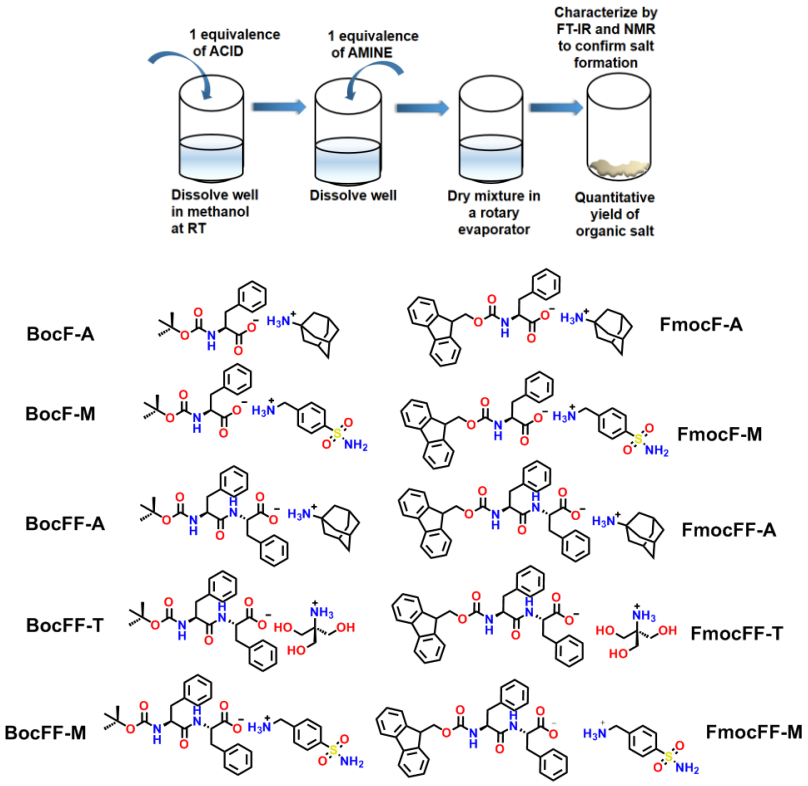

Scheme S2: Library of **PAM salts** studied

Physicochemical data:

BocFF: white solid; m.p. 72°C; yield 61-65% ; ^{1}H NMR (300 MHz, MeOD) δ ppm 7.21 (dt, *J* = 11.1, 5.2, 5.2 Hz, 10H), 4.69 – 4.50 (m, 1H), 4.25 (dt, *J* = 15.1, 7.5, 7.5 Hz, 1H), 3.17 (td, *J* = 14.1, 13.9, 6.9 Hz, 1H), 2.96 (dtt, *J* = 36.1, 13.9, 13.9, 6.5, 6.5 Hz, 2H), 2.77 – 2.55 (m, 1H), 1.30 (d, *J* = 14.7 Hz, 9H); ^{13}C NMR (75 MHz, MeOD) δ ppm 175.27, 174.21, 157.72, 138.92, 138.57, 138.39, 130.76, 130.58, 129.65, 129.61, 127.97, 127.87, 80.89, 57.60, 55.62, 39.42, 38.84, 34.99, 30.99, 28.93, 24.50. (Fig. S24). FT-IR (ν cm^{-1}) =1722 cm^{-1} (stretching frequency of >C=O$_{acid}$) 1692 cm^{-1} (stretching frequency of >C=O$_{carbamate}$), 1658 cm^{-1} (stretching frequency of >C=O$_{amide}$.); (Fig. S26) ESI-MASS: $C_{23}H_{28}N_2O_5$ calculated for $[M]^+$ at 412.4860 *m/z* and experimentally obtained for $[M+Na]^+$ at 435.0648 *m/z.* ((Fig. S27)

FmocFF: white solid; m.p. 150°C; yield 76-81 % ; ^{1}H NMR (300 MHz, MeOD) δ ppm 7.77 (d, *J* = 7.5 Hz, 2H), 7.54 (d, *J* = 7.4 Hz, 2H), 7.44 – 7.01 (m, 14H), 4.66 (dd, *J* = 8.1, 5.3 Hz, 1H), 4.48 – 3.95 (m, 4H), 3.25 – 2.87 (m, 3H), 2.74 (ddd, *J* = 25.6, 12.9, 8.8 Hz, 1H); ^{13}C NMR (75 MHz, MeOD) δ ppm 174.87, 173.70, 158.06, 145.10, 142.46, 138.57, 138.19, 130.38, 130.31, 129.39, 129.35, 128.72, 128.13, 127.76, 127.69, 126.27, 126.14, 120.86, 68.04, 57.67, 55.24, 39.14, 38.92, 38.48, 26.24. (Fig. S25) FT-IR (ν cm^{-1}) = 1710 cm^{-1} (>C=O$_{acid}$) 1690 cm^{-1} (>C=O$_{carbamate}$) 1653 cm^{-1} (>C=O$_{amide}$) (Fig. S28); ESI-MASS: $C_{33}H_{30}N_2O_5$ calculated for $[M]^+$ at 534.2231 *m/z* and obtained experimentally at $[M+Na]^+$ at 557.2051 *m/z.* (Fig. S29)

Salt BocF-A: white solid; m.p. 173°C; ^{1}H NMR (300 MHz, Methanol-d_4) δ ppm 7.19 (d, *J* = 9.9 Hz, 6H), 4.28 – 4.16 (m, 1H), 3.15 (dd, *J* = 13.6, 4.8 Hz, 1H), 2.90 (dd, *J* = 13.5, 7.6 Hz, 1H), 2.16 (s, 3H), 1.89 – 1.64 (m, 12H), 1.32 (d, *J* = 25.5 Hz, 9H); ^{13}C NMR (101 MHz, DMSO) δ ppm 173.88, 154.95, 139.05, 129.57, 127.88, 125.92, 77.68, 62.93, 56.18, 50.82, 40.21, 39.94, 39.73, 39.31, 39.10, 38.89, 37.53, 35.27, 28.53, 28.34. (Fig. S30) FT-IR (ν cm^{-1}) =1671 cm^{-1} (>C=O$_{carboxylate}$), 1636 cm^{-1} (>C=O$_{carbamate}$).

Salt BocF-M: pale-yellow solid; m.p. 85°C; ^{1}H NMR (300 MHz, Methanol-d_4) δ ppm 7.94 (d, *J* = 8.5 Hz, 2H), 7.60 (d, *J* = 8.5 Hz, 2H), 7.29 – 7.08 (m, 5H), 4.24 – 4.09 (m, 3H), 3.14 (dd, *J* = 13.6, 4.8 Hz, 1H), 2.89 (dd, *J* = 13.5, 7.5 Hz, 1H), 1.32 (d, *J* = 25.7 Hz, 9H); ^{13}C NMR (101 MHz, DMSO) δ ppm 174.18, 155.00, 143.51, 141.06, 138.94, 129.45, 128.85, 127.90, 125.93, 125.79, 77.67, 56.06, 42.61, 40.15, 39.94, 39.73, 39.31, 39.10, 38.89, 37.39, 28.30. (Fig. S31) FT-IR (ν cm^{-1}) = 1700 cm^{-1} (>C=O$_{carboxylate}$), 1688 cm^{-1} (>C=O$_{carbamate}$)

Salt BocFF-A: white solid; m.p. 100°C; ^{1}H NMR (300 MHz, MeOD) δ ppm 7.34 – 7.07 (m, 10H), 4.53 (d, *J* = 35.1 Hz, 2H), 4.38 – 4.09 (m, 1H), 3.27 – 2.82 (m, 3H), 2.82 – 2.55 (m, 1H), 2.16 (s, 2H), 1.95 – 1.54 (m, 8H), 1.30 (d, *J* = 11.7 Hz, 9H); ^{13}C NMR (75 MHz, DMSO) δ ppm 173.17, 170.63, 155.22, 138.79, 138.65, 129.76, 129.62, 129.14, 128.04, 127.95, 127.70, 126.11, 125.76, 56.50, 55.08, 50.41, 40.18, 37.43, 35.25, 28.42, 28.17. (Fig. S32) FT-IR (ν cm^{-1}) =1705 cm^{-1} (>C=O$_{carboxylate}$), 1692 cm^{-1} (>C=O$_{carbamate}$), 1653 cm^{-1} (>C=O$_{amide}$.).

Salt BocFF-T: white solid; m.p. 210°C; ^{1}H NMR (300 MHz, MeOD) δ ppm 7.18 (dd, *J* = 15.3, 4.3 Hz, 10H), 4.48 (dt, *J* = 19.9, 6.0, 6.0 Hz, 1H), 4.26 (ddd, *J* = 14.3, 10.0, 3.9 Hz, 1H), 3.61 (s, 8H), 3.27 – 2.89 (m, 3H), 2.78 – 2.51 (m, 1H), 1.40 – 1.17 (m, 10H); ^{13}C NMR (75 MHz, DMSO) δ ppm 174.47, 170.71, 155.27, 138.70, 129.81, 129.64, 129.21, 128.12, 128.01, 127.83, 126.19, 125.87, 78.27, 60.56, 59.93, 56.63, 55.27, 37.61, 28.23. (Fig. S33) FT-IR (ν cm^{-1}) = 1681 cm^{-1} (overlapped >C=O$_{carboxylate}$ and >C=O$_{carbamate}$), 1653 cm^{-1} (>C=O$_{amide}$).

Salt BocFF-M: pale-yellow solid; m.p. 112°C; ^{1}H NMR (300 MHz, MeOD) δ ppm 7.89 (d, *J* = 8.4 Hz, 3H), 7.54 (d, *J* = 8.4 Hz, 3H), 7.18 (dq, *J* = 12.8, 5.0, 5.0, 4.2 Hz, 10H), 4.55 – 4.39 (m, 1H), 4.23 (dd, *J* = 10.1, 3.8 Hz, 1H), 3.99 (s, 3H), 3.27 – 2.93 (m, 3H), 2.75 – 2.54 (m, 1H), 1.37 – 1.16 (m, 9H); ^{13}C NMR (75 MHz, DMSO) δ ppm 173.66, 170.66, 155.27, 144.23, 142.89, 138.84, 138.66, 129.78, 129.63, 129.18, 128.22, 128.08, 127.76, 126.15, 125.80, 125.67, 78.18, 56.53, 55.21, 43.66, 40.36, 40.08, 39.80, 39.52, 39.24, 38.96, 38.68, 37.46, 28.20, 27.83. (Fig. S34) FT-IR (ν cm^{-1}) = 1693 cm^{-1} (overlapped >C=O stretching frequency of >C=O$_{carboxylate}$ and >C=O$_{carbamate}$), 1654 cm^{-1} (>C=O$_{amide}$).

Salt FmocF-A: white solid; m.p. 152.5°C; ^{1}H NMR (300 MHz, Methanol-d_4) δ ppm 7.77 (d, *J* = 7.5 Hz, 2H), 7.58 (dt, *J* = 9.1, 4.5 Hz, 2H), 7.42 – 7.09 (m, 10H), 4.40 – 4.05 (m, 5H), 3.20 (dd, *J* = 13.6, 4.6 Hz, 1H), 2.93 (dd, *J* = 13.6, 8.1 Hz, 1H), 2.14 (s, 3H), 2.03 – 1.56 (m, 12H); ^{13}C NMR (151 MHz, DMSO) δ ppm 173.16, 155.24, 144.00, 142.60, 140.73, 139.46, 129.50, 129.43, 128.99, 127.76, 127.63, 127.36, 127.10, 127.08, 125.74, 125.34, 125.23, 121.46, 120.14, 120.10, 109.88, 65.26, 56.82, 50.20, 46.75, 40.62, 39.94, 39.80, 39.66, 39.38, 39.25, 39.11, 37.44, 35.28, 28.45. (Fig. S35). FT-IR (ν cm^{-1}) =1725 cm^{-1} (>C=O$_{carboxylate}$), 1688 cm^{-1} (>C=O$_{carbamate}$).

Salt FmocF-M: pale-yellow solid; m.p. 165°C; ^{1}H NMR (300 MHz, Methanol-d_4) δ ppm 7.93 (d, *J* = 8.4 Hz, 2H), 7.76 (d, *J* = 7.5 Hz, 2H), 7.58 (d, *J* = 8.3 Hz, 4H), 7.46 – 7.04 (m, 10H), 4.41 – 4.03 (m, 6H), 3.18 (dd, *J* = 13.6, 4.6 Hz, 1H), 2.94 (td, *J* = 13.6, 12.0, 6.9 Hz, 1H). ^{13}C NMR (101 MHz, DMSO) δ 173.74, 157.51, 155.49, 144.63, 143.91, 142.65, 140.76, 139.50, 137.51, 129.44, 129.04, 128.39, 127.91, 127.35, 127.16, 126.53, 125.72, 125.26, 121.46, 120.10, 109.79, 65.43, 56.70, 55.64, 46.78, 43.49, 37.42, 37.04. (Fig. S36) FT-IR (ν cm^{-1}) =1716 cm^{-1} (>C=O$_{carboxylate}$), 1695 cm^{-1} (>C=O$_{carbamate}$).

Salt FmocFF-A: white solid; m.p. 92.5°C; ^{1}H NMR (300 MHz, MeOD) δ ppm 7.75 (t, *J* = 7.7, 7.7 Hz, 2H), 7.53 (d, *J* = 7.2 Hz, 2H), 7.36 (t, *J* = 7.4, 7.4 Hz, 3H), 7.18 (qt, *J* = 16.1, 16.1, 16.1, 7.1, 7.1 Hz, 14H), 4.50 (s, 1H), 4.29 (ddd, *J* = 24.6, 10.2, 5.1 Hz, 2H), 4.10 (q, *J* = 11.0, 8.8, 8.8 Hz, 2H), 3.24 – 2.97 (m, 3H), 2.73 (dd, *J* = 27.6, 14.0 Hz, 1H), 2.14 (s, 3H), 1.88 – 1.65 (m, 12H); ^{13}C NMR (75 MHz, DMSO) δ ppm 173.44, 171.06, 157.05, 142.64, 139.49, 138.71, 137.49, 129.71, 129.21, 128.99, 128.07, 127.75, 127.35, 126.12, 125.81, 121.43, 120.07, 109.76, 56.84, 55.11, 50.47, 37.58, 35.24, 28.43. (Fig. S37) FT-IR (ν cm^{-1}) = 1695 cm^{-1} (overlapped >C=O$_{carboxylate}$ and >C=O$_{carbamate}$), 1645 cm^{-1} (>C=O$_{amide}$.)

Salt FmocFF-T: white solid; m.p. 105°C; ^{1}H NMR (300 MHz, MeOD) δ ppm 7.76 (d, *J* = 7.5 Hz, 2H), 7.53 (d, *J* = 6.8 Hz, 1H), 7.36 (t, *J* = 7.4, 7.4 Hz, 2H), 7.20 (tp, *J* = 16.5, 16.5, 9.4, 9.4, 8.3, 8.3 Hz, 13H), 4.50 (s, 1H), 4.39 – 4.17 (m, 2H), 4.10 (q, *J* = 10.7, 8.7, 8.7 Hz, 2H), 3.65 (s, 7H), 3.27 – 2.92 (m, 3H), 2.84 – 2.60 (m, 1H); ^{13}C NMR (101 MHz, DMSO) δ ppm 174.32, 172.86, 142.67, 139.51, 138.69, 137.52, 129.72, 129.48, 129.24, 129.06, 128.35, 128.14, 127.76, 127.42, 126.32, 125.86, 121.47, 120.11, 109.81, 60.41, 60.11, 56.90, 56.09, 55.31, 54.74, 47.67, 46.62, 40.58, 37.73, 33.43, 32.34, 25.30, 24.56. (Fig. S38) FT-IR (ν cm^{-1}) = 1693 cm^{-1} (overlapped >C=O$_{carboxylate}$ and >C=O$_{carbamate}$), 1643 cm^{-1} (>C=O$_{amide}$.)

Salt FmocFF-M: pale yellow solid; m.p. 118°C; ^{1}H NMR (300 MHz, MeOD) δ 7.95 (d, *J* = 7.5 Hz, 2H), 7.76 (d, *J* = 7.5 Hz, 3H), 7.56 (dd, *J* = 20.4, 7.4 Hz, 4H), 7.35 (d, *J* = 7.5 Hz, 2H), 7.21 (dt, *J* = 15.3, 6.6, 6.6 Hz, 15H), 4.51 (s, 1H), 4.36 – 4.21 (m, 2H), 4.19 – 4.05 (m, 5H), 3.23 – 2.97 (m, 3H), 2.73 (dd, *J* = 28.1, 14.8 Hz, 1H). ^{13}C NMR (101 MHz, DMSO) δ 173.74, 172.41, 166.39, 157.53, 144.65, 142.67, 139.52, 137.53, 129.95, 129.51, 129.05, 128.34, 127.89, 127.42, 126.66, 125.76, 121.47, 120.11, 55.57, 43.50, 42.78, 37.59, 33.42, 25.41, 24.55. (Fig. S39) FT-IR (ν cm^{-1}) = 1693 cm^{-1} (overlapped >C=O$_{carboxylate}$ and >C=O$_{carbamate}$), 1644 cm^{-1} (>C=O$_{amide}$.)

Gelation, M.G.C measurements and T_{gel} Experiments: The pure hydrogels as well as organogels (at 4 wt % w/v i.e 40 mg of compound in 1ml of solvent) were prepared by solubilising the organic salts in the corresponding solvents by heating so that they form clear solutions and the solutions were kept at room temperature until gels were formed (Figure S5) . In case of pure hydrogels initial solutions during heating appeared to be little turbid which subsequently formed gels. Complete gel formation was ensured by vial-inversion technique where gels were able to sustain their own weight against gravity. The minimum gelator concentration (M.G.C) of the hydrogels and methyl salicylate gels was determined by performing gelation with sets of decreasing gelator concentrations and the optimum concentration in wt % was recorded beyond which no stable gel formation was observed. The T_{gel} or Gel to Sol dissociation temperature for various gelator concentrations, including M.G.C, was measured by dropping-ball method. In this method, a glass ball, weighing 229 mg, was placed cautiously on the surface of a 0.5 mL gel preformed in a glass vial. The glass vial was then immersed in an oil bath and the gel was gradually heated until the glass ball penetrated through the dissociating gel phase with

increasing temperature (monitored by a thermometer) and finally touched the bottom of the vial. The temperature at which the ball touched the bottom of the vial was noted.

Rheology sample preparation: For rheological experiments, gels were freshly prepared at a standard concentration of 4 wt % in the respective solvents (pure water and methyl salicylate). Rheological studies were carried out with an Anton Paar Modular Compact Rheometer MCR 102 at 25°C in parallel-plate geometry (25 mm diameter, 1 mm gap). In one such experiment, 1.5 mL (approximately) of gel sample was placed carefully on the stationary plate and variations of both strain and angular frequency was employed over the particular gel sample by the parallel non-stationary plate for the amplitude and frequency sweep experiment respectively.

TEM sample preparation: Hydrogels (1 mL in pure water at M.G.C) were freshly prepared in vials and very small amount of these gels were uniformly smeared on carbon-coated Cu TEM grid (300 mesh) with the help of a flat spatula. The TEM grids were then air-dried under ambient conditions. Following TEM experiment was carried out at an accelerating voltage of 200 kV without staining.

Single Crystal X-ray Diffraction: Appropriate single and diffraction quality crystals of **BocF-A**, **FmocF-M**, **FmocF-A** and **BocF-M** were obtained by slowly evaporating the corresponding solution of the salt in organic solvents (Table S3). Gradual dissociation (within 2-3 days) of the methyl salicylate gel of **BocF-M** resulted in crystals, out of which, a suitable single crystal was selected for SXRD. Data was collected in two different diffractometers (Bruker APEX III D8 Venture, PHOTON II detector, MoKα, λ = 0.7107 and Bruker APEX II, CCD area detector, Mo K*α*, λ= 0.7107 Å). Data collection, data reduction and structure solution were performed in APEX-III software package. Subsequent data refinement and CIF finalisation procedures were carried out in OLEX2 version 1.3. The non-hydrogen atoms were refined anisotropically. CCDC-numbers **2190086**, **2190087**, **2190088**, **2190089** contain the crystallographic data for **FmocF-A**, **BocF-M**, **BocF-A**, and **FmocF-M** respectively.

Powder X-ray Diffraction: PXRD data of the bulk and xerogel samples were recorded using Rigaku Smartlab (40 kV, 110 mA, Cu Kα1 radiation, λ= 1.5406 Å, step size = 0.010). Bulk samples were prepared by grinding the corresponding crystals into fine powder. Xerogel samples were obtained by complete drying of the gels and grinding the dried gels into powder. Approximately 15 mg of these samples taken for the PXRD experiment with a scan speed of for a scan range of 4°−40° (2θ). Simulated PXRD patterns were generated from the CIFs using Mercury 3.8 software.

Temperature dependent NMR spectroscopy: 600 μl of hydrogels of **FmocFF-T** and **FmocFF-M** was prepared in NMR tubes at their respective M.G.Cs i.e. at 2 wt % and 1.5 wt %. In the V-T (variable temperature) mode of the NMR experiment, temperatures of the gel sample was gradually increased from 25°C (RT) to 85°C (high temperature) and the ^{1}H NMR of the sample was collected at each temperature stops with the same no. of scans.

Anti-Bacterial activity by Zone Inhibition: 100 μL of log-phase bacterial solution ((*E. coli*, ≈3 × 107 cfu/mL)), initially incubated in nutrient broth media at 37 °C in a BOD shaker incubator for 24 hours, was inoculated uniformly on an agar-plate by the help of a glass spreader. For introducing the compounds, 4 grooves were cut out of the agar plate at well separated distances by the wide end of a sterile 1 mL microtip. For studying Zone-inhibition properties of the hydrogel, 500 μL of 4 wt % **FmocFF-M** hydrogel was introduced in a groove cut on the nutrient agar plate along with the positive control Mafenide and was observed after 24 h of incubation. The agar-plate was placed in the incubator for 24 h at 37 °C. The bacteria zone inhibition diameters was measured after the given time with the help of a scale.

MIC (Minimum Inhibitory Concentration) determination: In Turbidity assay, bacterial cells (*E. coli*, *S. aureus* and *P. auregonisa*) were primarily grown in a nutrient broth media at 37 °C in a BOD shaker incubator. After 6 h, while bacterial cells were at the log phase, absorbance of the culture was measured at 600 nm (i.e., initial OD_{600}). Cultured bacterial suspension (200 μL) collect at log phase was treated with varying concentration of FmocFF-M in a 96-well plate. For each concentration of

FmocFF-M, three experiments were performed. The well plate was then incubated in a BOD shaker at 37^0C for 24 h and OD_{600} of each well was measured using a 96-well plate reader to determine MIC. The bacterial cell growth inhibition and MIC was also studied by Resazurin assay. In this case, each well was treated with varying concentration of FmocFF-M along with Resazurin (10 μL taken from a 5 mg/mL stock solution) and the well plate was incubated for 2 h in a BOD shaker at 37^0C following which colour of the wells was noted (Fig. S17).

Bacterial Growth curve experiment: 50 μl of initially cultured log-phase bacteria (*E.coli* and *P. aerugonisa*) was inoculated in 6 mL of nutrient broth medium. Different sets of these bacterial suspension was treated with varying concentration of **FmocFF-M** and the OD_{600} values of the individual sets were measured at regular time intervals for 36 h. The OD_{600} vs Time curves were plotted for the control set and for the individual sets of concentrations of **FmocFF-M** (Fig. S18).

Bacterial SEM experiment: Initially cultured log phase bacteria (***E. coli***) taken in broth media in a 15 mL falcon was treated with 100 μg/mL DMSO solution of **FmocFF-M** and incubated for 12 h. The bacterial solution was then centrifuged (at 12000 r.p.m. for 15 mins) and the precipitated **FmocFF-M** treated bacterial cells was collected and washed thrice with PBS. The cells were subsequently fixed in 4% glutaraldehyde solution. The fixed cells was then washed with excess PBS to drain extra amount of glutaraldehyde. The resultant bacterial precipitate was further washed with increasing concentrations of ethanol and in the final step, a bacterial suspension is prepared in 100 % ethanol. 10 μL of this solution is drop-casted on a glass cover slip and dried in the incubator at 37°C, placed on the SEM stub and SEM images were recorded.

Bacterial cell death mechanism by Flow Cytometry: Plausible mechanism of bacterial cell death was investigated by Flow cytometry under different staining conditions (Propidium iodide and DCFDA). In a typical experiment, early log-phase bacteria (***E. coli***) (990 μL) was treated with DMSO solution of **FmocFF-M** (10 μL of 10 mg/mL) so that the final concentration of **FmocFF-M** reached 100 μg/mL and then incubated in a BOD shaker for 2 h. The control experiment consisted of the same bacterial solution with equivalent amount of DMSO. After 2 h, the control and drug-treated bacterial cells were individually treated with PI dye (final concentration 10 μg/mL) and DCFDA (final concentration 5mM). Both the solutions were further incubated for 15 mins at 37 °C. The cells were then centrifuged, collected in a falcon tube and washed several times with PBS to get rid of the excess dye. The dye-stained cells were finally taken in 1 mL of PBS, shaked well and studied by FACS in a BD LSRFortessa flow cytometer. (Fig. S19). Same experiments were performed with ***E.derm*** with DCFDA staining to assess the accumulation of ROS. (Fig. S21)

MTT assay: ***E. derm*** cells**,** cultured in low-glucose Dulbecco's modified Eagle's medium (DMEM) supplemented with 10 % fetal bovine serum (FBS),1% penicillin-streptomycin and a mixture of non-essential amino acids, were seeded in a 96 well plate and kept in incubation (37 °C under 5% CO_2 atmosphere) for 24 h. The media was then discarded and varying concentration of **FmocFF-M (**150 μl) was then added to the adhered cells. After 24 h of incubation, the media was discarded and to each well, MTT (100 μL of 0.5 mg/mL MTT solution in DMEM) was added followed by 4 h of incubation. After discarding the media, DMSO (100 μL) was added to each well and reading was taken in ELISA reader. Similar procedure was performed to carry out MTT assay on HEK 293 cell line. Note that HEK 293 cells were cultured in a similar fashion except that in this case, high-glucose Dulbecco's modified Eagle's medium (DMEM) was used and addition of non-essential amino acids was omitted (Fig. S20).

Hemolysis experiment: In a typical experiment, fresh blood sample was collected from healthy BALB/c mice with body weight of about 20 g by cardiac-puncture method, followed by treatment of EDTA solution to avoid coagulation. Experiments were carried out under the ethical guidelines approved by IAEC permission (IACS/IAEC/-2021-01). 1 mL of these blood sample was diluted in PBS up to a final volume of 10 mL and the resultant solution was centrifuged to precipitate out the red blood cells (RBC) (3000 r.p.m for 10 mins). The precipitated cells were washed few times with PBS and a final stock solution of 10 % (v/v) of the blood cells in PBS was prepared. 1 ml from this solution was

introduced in different Eppendorf tube (1.5 ml), treated with different concentrations of **FmocFF-M** (50 μg/mL to 200 μg/mL) and the positive control of 0.1% SDS solution. The colours of the drug-treated wells were observed (after 2 h of incubation) in comparison to the positive control (SDS) which caused complete disruption of the RBCs and the appearance of dark-red colouration. The Eppendorf were then centrifuged to precipitate down the unruptured RBCs and photograph was recorded to observe a visual depiction of the extent of hemolysis. Further, the soups from the Eppendorf were collected and the OD_{540} values were recorded. The absorbance (OD_{540}) values of the wells were measured and plotted as a function of **FmocFF-M** concentrations. The %hemolysis was calculated by considering the positive control (0.1 % SDS) as 100%. To evaluate the hemolytic behaviour of **FmocFF-M** hydrogel (4 wt% or 40 mg/mL), PBS suspension of RBCs was carefully topped on a 500μl, 4 wt% **FmocFF-M** hydrogel bed, incubated for 2 h, and the OD_{540} values of the supernatant was measured. Experiments were done in triplicate to ensure reproducibility of the results (see Fig. S22).

Drug-leaching Experiment: 1 mL hydrogel of **FmocFF-M** at 4 wt % was prepared and carefully topped with 1 mL of distilled water. The gel was then kept under incubated conditions for 24 h at 37^0C. Drug release data was taken by collecting 100μL aliquots of aqueous layer at regular intervals of time and each time the volume was refilled up to 1 mL of distilled water. Quantitative estimation of drug leached into the aqueous layer was monitored by UV-vis spectroscopy where 100 μL aliquot of supernatant was diluted thrice, 20 μL of the resultant solution was added in 1 mL of water and the Absorbance value was measured. (Fig. S23)

Rheoreversibility experiment: 4 wt % hydrogel of **FmocFF-M** was subjected to cycles of variable shear strains and the rheo-reversibility character was studied. Initially, the hydrogel sample was sheared with low amplitude of γ = 0.1% (as indicated as LVE strain from previous amplitude sweep experiment) for 120 s (10 s for each of 12 measuring points) with angular frequency of 10 rad/s. The same sample was then applied with high strain amplitude of γ = 30% (which is much greater than the proposed LVE range) with same angular frequency of 10 rad/s for 120 s

Real-life topical application of hydrogel: 15 mL 4 wt % solution of **FmocFF-M** in distilled water was heated till it attained a turbid solution. This hot solution was then loaded into a plastic tube through the previously cut wide-end of the tube and was allowed to cool to room temperature. Gel formation was confirmed by inversion of the tube which showed no gel deformation. The wide end was then sealed and the tube was squeezed by hand. Easy release of the hydrogel from the tube was observed without any phase separation problem (**Video** in Supporting Information, ESI†)

Statistical Analysis: All experiments were performed in triplicate (n = 3). Column heights designate mean values and bars represent SD values. Comparisons between two groups were determined by t tests. In case of more than two groups, one-way ANOVA was performed and differences at $P < 0.05$ were considered statistically significant by Duncan multiple range tests. All data are represented as mean ± SD, where *P < 0.05, **P < 0.01, ***P < 0.001, and ns represents not significant. All data were analyzed by GraphPad PRISM (ver. 5.03)

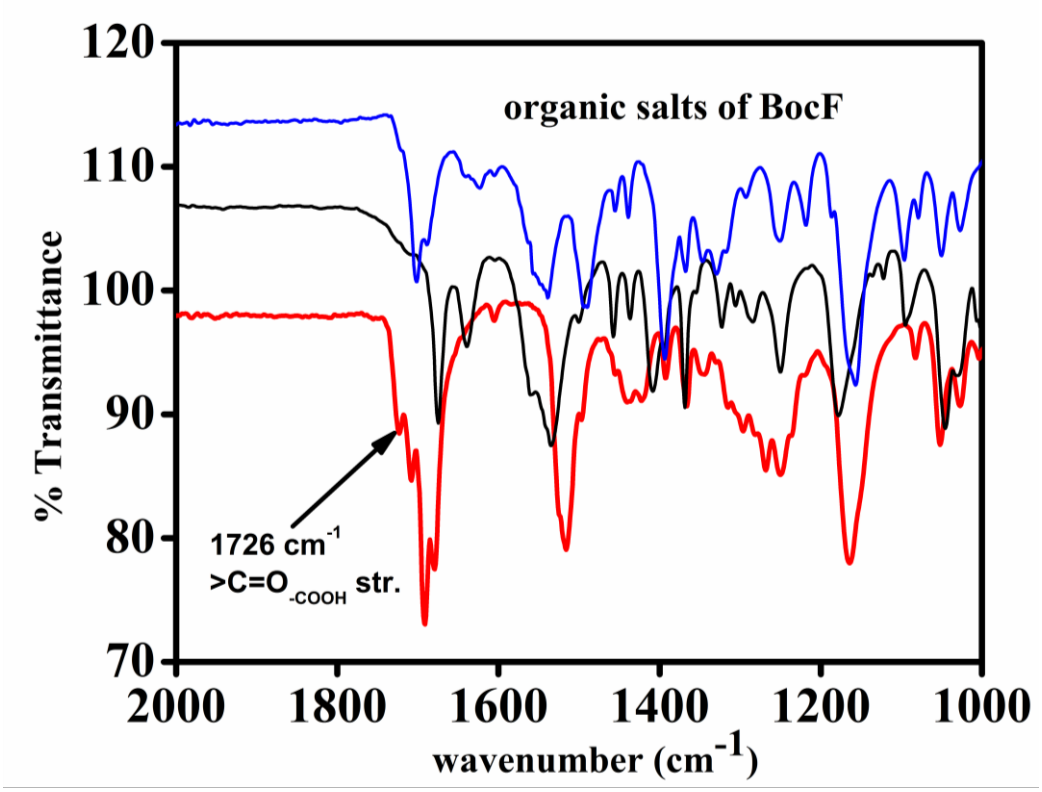

Fig. S1: FT-IR spectra of **BocF** (red) and its organic salts **BocF-A** (black) **and BocF-M** (blue)

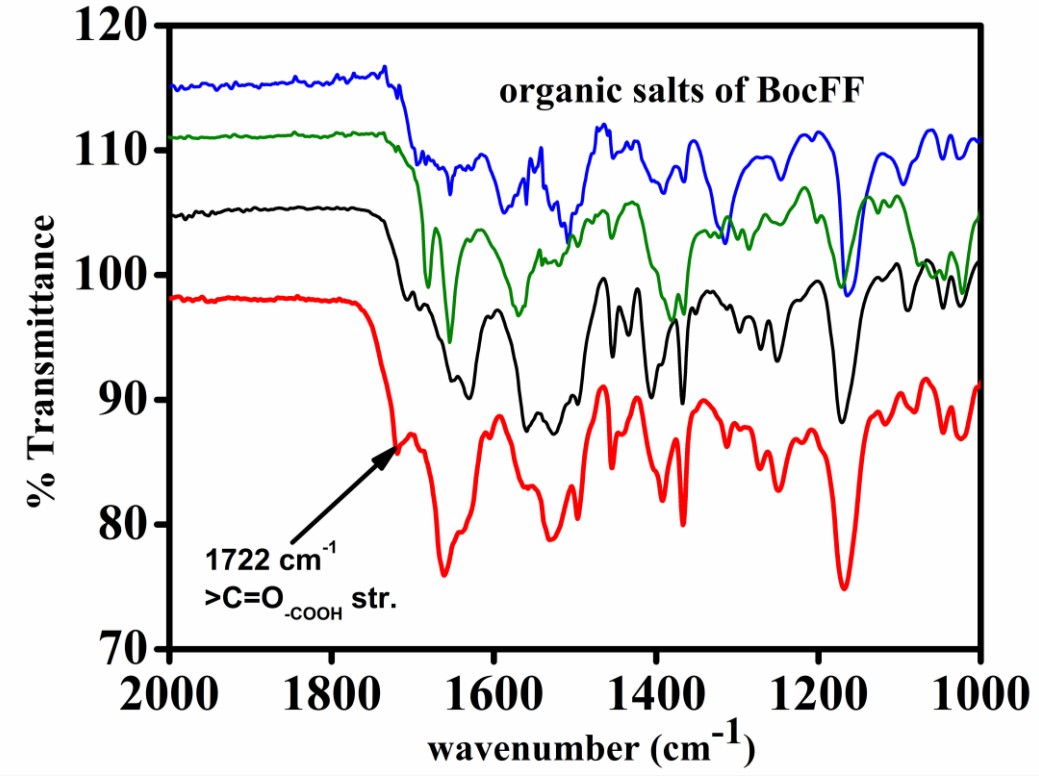

Fig. S2: FT-IR spectra of **BocFF** (red) and its organic salts **BocFF-A** (black), **BocFF-T** (blue) **and BocFF-M** (green)**.**

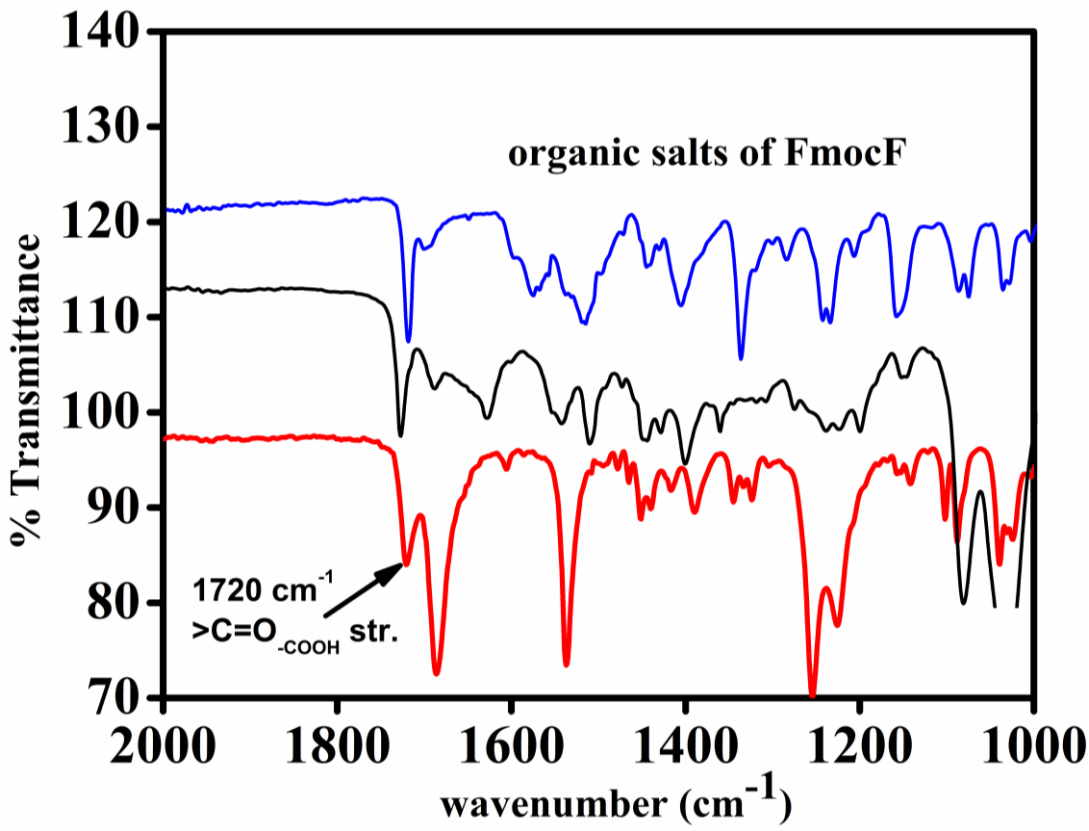

Fig. S3: FT-IR spectra of **FmocF** (red) and its organic salts **FmocF-A** (black) **and FmocF-M** (blue)

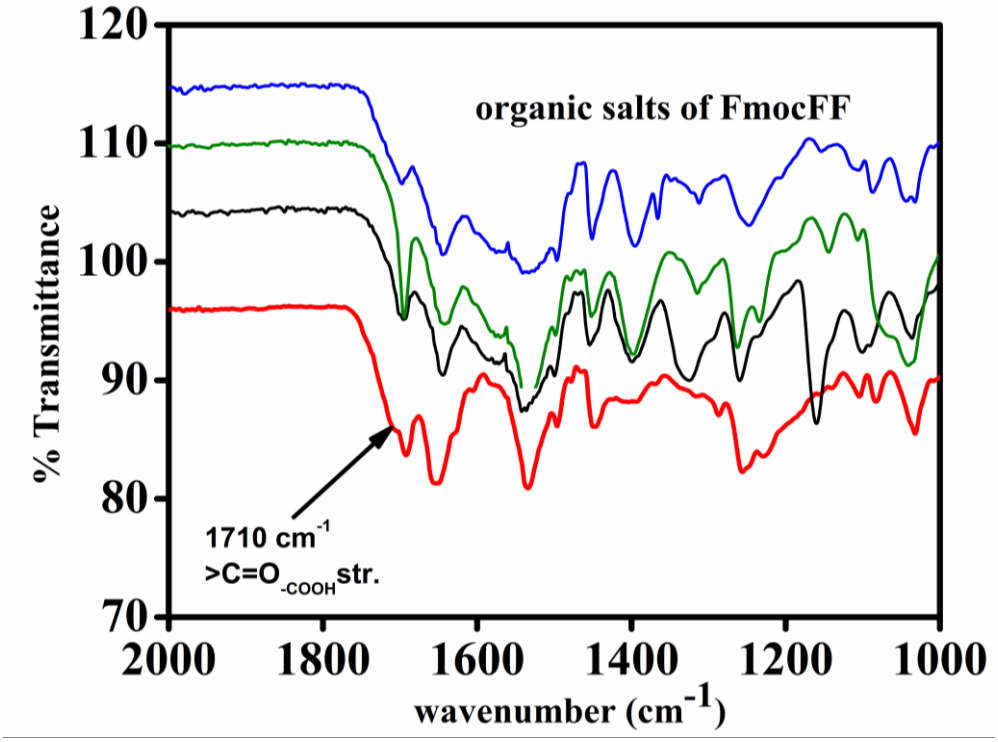

Fig. S4: FT-IR spectra of **FmocFF** (red) and its organic salts **FmocFF-A** (black)**, FmocFF-T** (blue) **and FmocFF-M** (green).

Table S1: Gelation table of all PAM salts under study in various solvents

Gelation solvents	BocF-A	BocF-M	FmocF-A	FmocF-M	BocFF-A	BocFF-T	BocFF-M	FmocFF-A	FmocFF-T	FmocFF-M
Pure Water	P	S	INS	GP	INS	TS	CS	CS	G	G
Methyl-salicylate	WG	G	GP	GP	S	PS	G	S	G	G
Bromobenzene	GP	WG	P	P	WG	CS	S	G	WG	P
Chlorobenzene	GP	WG	P	P	WG	PS	S	S	PS	S
1,2 Dichlorobenzene	S	G	P	WG	WG	G	S	S	PS	WG
Toluene	S	S	GP	P	G	PS	INS	WG	P	INS
o-xylene	GP	GP	WG	P	G	PS	S	WG	P	P
m-xylene	GP	GP	WG	P	G	PS	PS	WG	P	INS
p-xylene	GP	GP	WG	P	G	PS	S	WG	P	INS
Mesitylene	WG	S	G	P	G	S	S	WG	S	INS
Nitrobenzene	WG	G	GP	P	S	G	S	CS	G	WG
1,4 dioxane	S	S	INS	S	S	S	S	S	S	S
DMF	S	S	S	S	S	S	S	S	S	CS
DMSO	S	S	S	S	S	S	S	S	S	S
EG	S	S	S	S	S	S	S	S	S	S
Acetonitrile	S	S	S	S	P	P	P	PS	PS	P
THF	S	S	S	S	S	CS	P	S	PS	P
Water/DMSO(9:1)	P	S	P	GP	PS	S	S	WG	G	G
Water/EG(9:1)	P	S	P	P	S	S	S	P	G	G

Pure hydrogels | Methyl salicylate gels | Other organogels

P=precipitate; S= soluble; INS=insoluble; GP= gelatinous precipitate; CS= colloidal solution; G= gel; WG= weak gel; PS= partially soluble

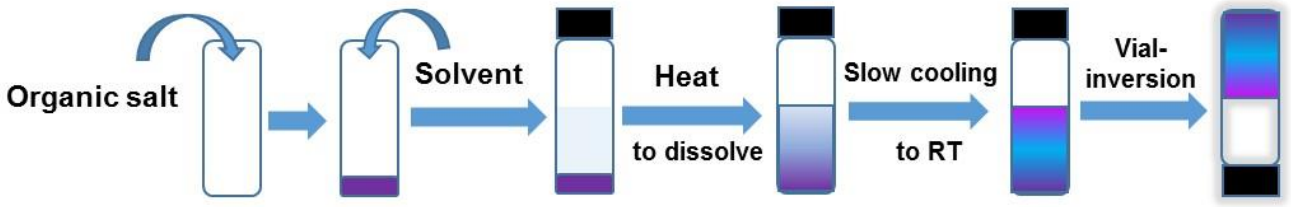

Fig. S5: Gelation procedure by **heat-cool method**

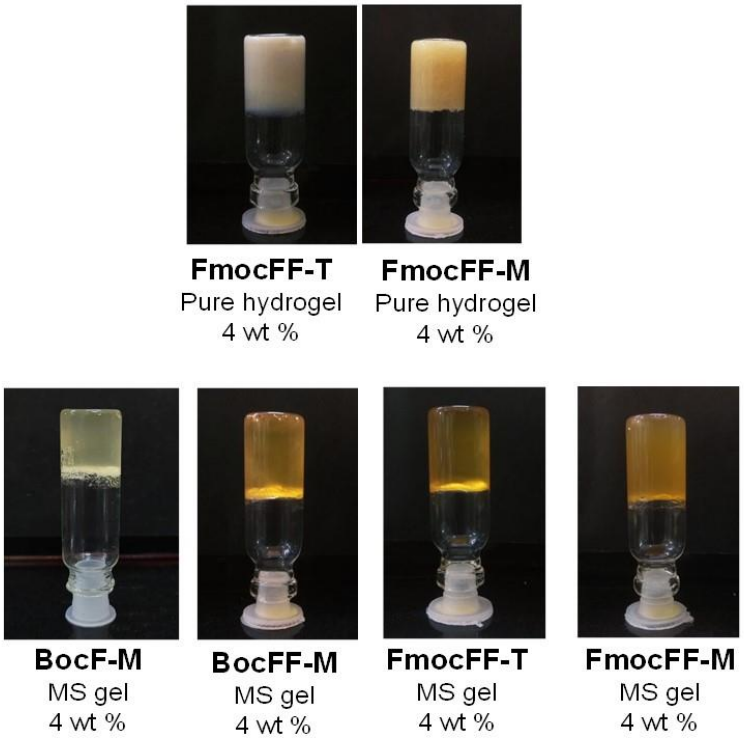

Fig. S6: Inverted-vial photographs of the hydrogels and MS (methyl salicylate) gels

Table S2: M.G.C and T_{gel} table for the hydrogels and MS gels

Salts	Gelation Solvents	Minimum Gelation Conc. (M.G.C)	T_{gel} average (at 4 wt %) (in °C)
FmocFF-T	Pure Water	**2 wt %** (20 mg/mL)	**106.6**
FmocFF-M	Pure Water	**1.5 wt %** (15 mg/mL)	**114.6**
BocF-M	Methyl salicylate	**1 wt %** (7.5 mg/mL)	**77.3**
BocFF-M	Methyl salicylate	**0.8 wt %** (8 mg/mL)	**78.6**
FmocFF-T	Methyl salicylate	**0.9 wt %** (9 mg/mL)	**69.3**
FmocFF-M	Methyl salicylate	**0.7 wt %** (7 mg/mL)	**102.6**

T_{gel}= Gel to Sol transition temperatures of the gels

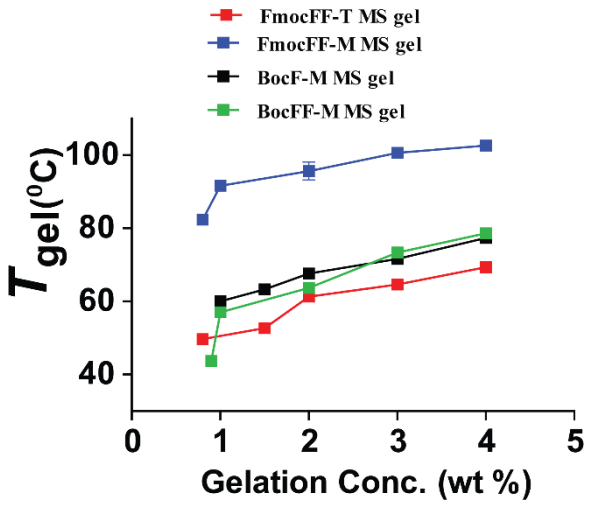

Fig. S7: T_{gel} versus [gelator] for the MS gels

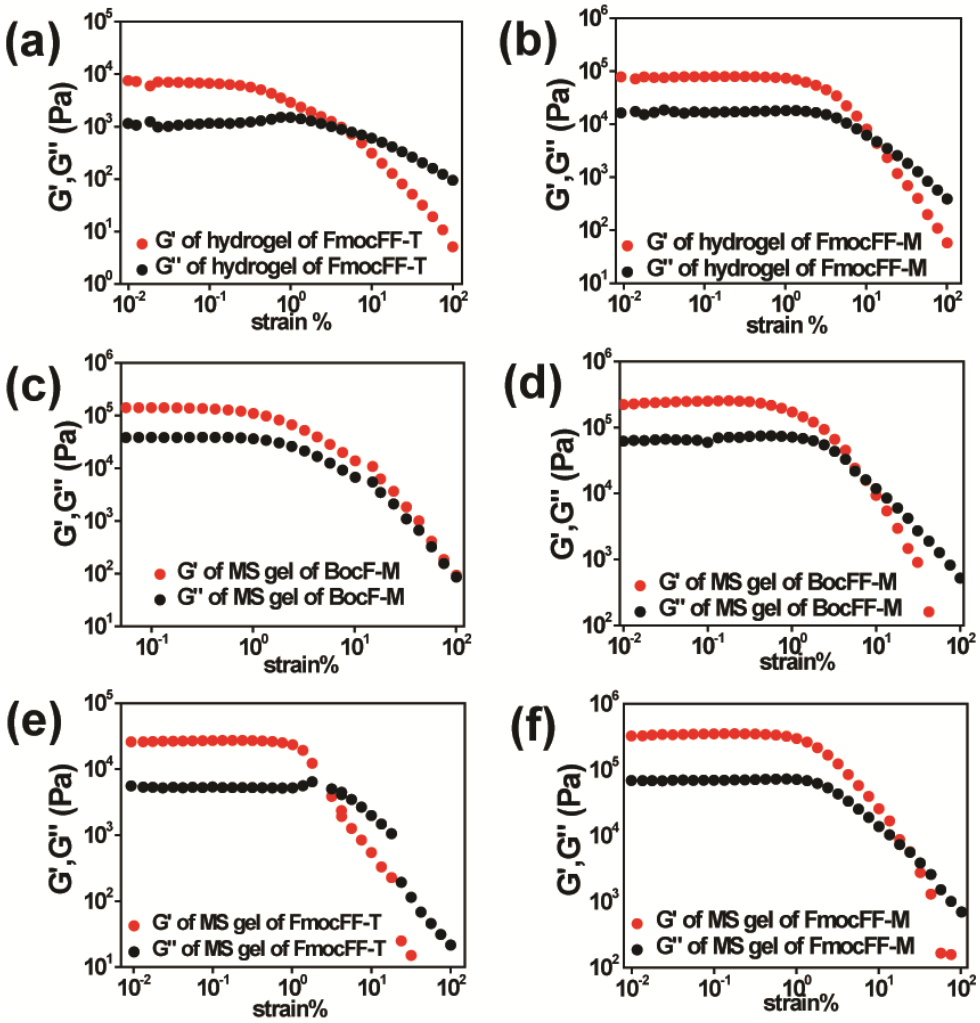

Fig. S8: Amplitude-sweep experiments of **4 wt%** gels: **(a) FmocFF-T** hydrogel, **(b) FmocFF-M** hydrogel, **(c) BocF-M** MS gel, **(d) BocFF-M** MS gel, **(e) FmocFF-T** MS gel, **(f) FmocFF-M** MS gel

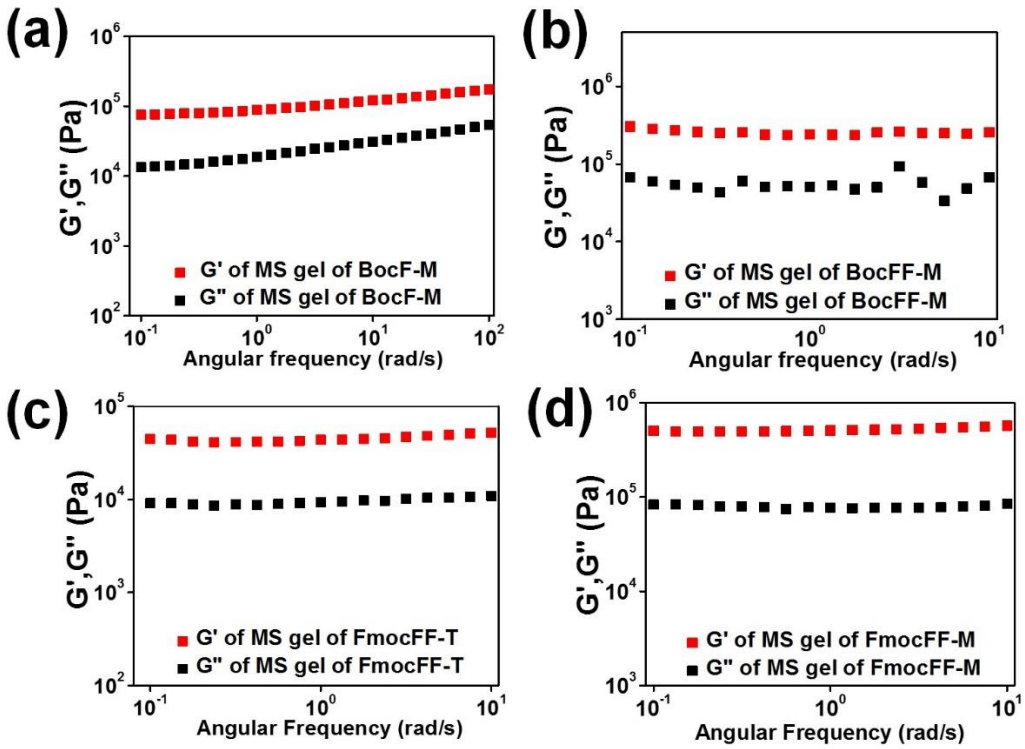

Fig. S9: Frequency-sweep experiments of **4 wt% MS** gels :**(a) BocF-M** MS gel, **(b) BocFF-M** MS gel, **(c) FmocFF-T** MS gel, **(d) FmocFF-M** MS gel

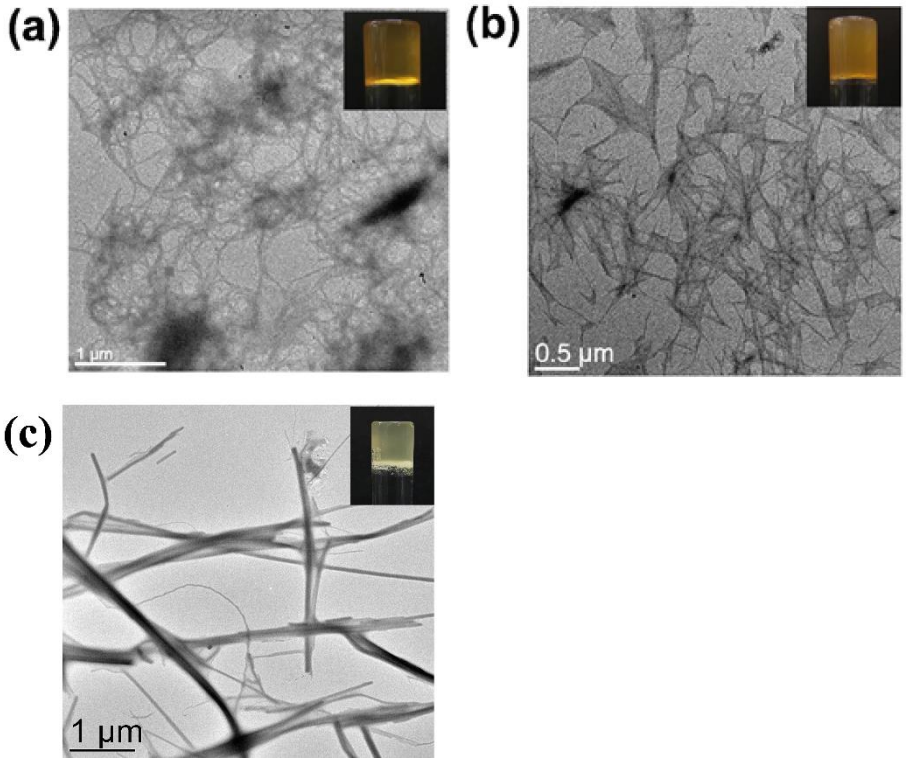

Fig. S10: TEM images of **(a) FmocFF-T** MS gel at M.G.C **2 wt% (b) FmocFF-M** MS gel at M.G.C **1.5 wt% (c) BocF-M** MS gel at M.G.C **2 wt%**

Table S3: Crystallographic data table:

Identification Code	BocF-A	BocF-M	FmocF-A	FmocF-M
Crystallizing solvent	DMSO solution	Methyl salicylate gel	EtOH+Et_2O mixture	EtOH+CH_3NO_2 mixture
Empirical formula	$C_{24}H_{36}N_2O_4$	$C_{21}H_{29}N_3O_6S$	$C_{34}H_{38}N_2O_4$	$C_{31}H_{31}N_3O_6S$
CCDC number	2190088	2190087	2190086	2190089
Formula weight	416.55	451.53	536.65	573.65
Temperature/K	296.15	197.48	144.98	259.84
Crystal system	monoclinic	monoclinic	monoclinic	monoclinic
Space group	$P2_1$	$P2_1$	$P2_1$	$P2_1$
a/Å	13.423(14)	10.809(4)	13.381(5)	12.229(5)
b/Å	6.446(7)	6.008(2)	6.665(2)	5.6301(17)
c/Å	13.679(15)	17.143(6)	15.732(5)	20.557(6)
α/°	90	90	90	90
β/°	95.363(16)	104.532(11)	94.009(9)	101.471(11)
γ/°	90	90	90	90
Volume/$Å^3$	1178(2)	1077.6(7)	1399.6(8)	1387.1(8)
Z	2	2	2	2
$\rho_{calc}g/cm^3$	1.174	1.392	1.273	1.373
μ/mm^{-1}	0.079	0.194	0.083	0.167
F(000)	452.0	480.0	572.0	604.0
Crystal size/mm^3	0.4 × 0.03 × 0.02	0.1 × 0.03 × 0.01	0.3 × 0.03 × 0.02	0.4 × 0.03 × 0.02
Radiation	MoKα (λ = 0.71073)	MoKα (λ = 0.71073)	MoKα (λ = 0.71073)	MoKα (λ = 0.71073)
2Θ range for data collection/°	2.99 to 51.706	4.91 to 50.738	5.192 to 50.03	4.736 to 69.116
Index ranges	-16 ≤ h ≤ 15, -7 ≤ k ≤ 7, -16 ≤ l ≤ 16	-12 ≤ h ≤ 12, -7 ≤ k ≤ 7, -20 ≤ l ≤ 20	-14 ≤ h ≤ 15, -7 ≤ k ≤ 5, -18 ≤ l ≤ 18	-17 ≤ h ≤ 18, -8 ≤ k ≤ 8, -32 ≤ l ≤ 29
Reflections collected	17464	10667	6685	19426
Independent reflections	4396 [R_{int} = 0.0955, R_{sigma} = 0.0869]	3761 [R_{int} =0.1240, R_{sigma} = 0.1573]	3671 [R_{int} = 0.1267, R_{sigma} = 0.2489]	9353 [R_{int} = 0.1014, R_{sigma} = 0.1834]
Data/restraints/parameters	4396/1/276	3761/1/285	3671/2/363	9353/1/380

Goodness-of-fit on F^2	**0.901**	**0.989**	**0.958**	**1.016**
Final R indexes [I>=2σ (I)]	**R_1 = 0.0544, wR_2 = 0.1252**	**R_1 = 0.0634, wR_2 = 0.1173**	**R_1 = 0.1004, wR_2 = 0.2064**	**R_1 = 0.0748, wR_2 = 0.1384**
Final R indexes [all data]	**R_1 = 0.1216, wR_2 = 0.1584**	**R_1 = 0.1292, wR_2 = 0.1519**	**R_1 = 0.2450, wR_2 = 0.2717**	**R_1 = 0.1869, wR_2 = 0.1847**
Largest diff. peak/hole / e $Å^{-3}$	**0.17/-0.19**	**0.29/-0.37**	**0.18/-0.19**	**0.36/-0.37**

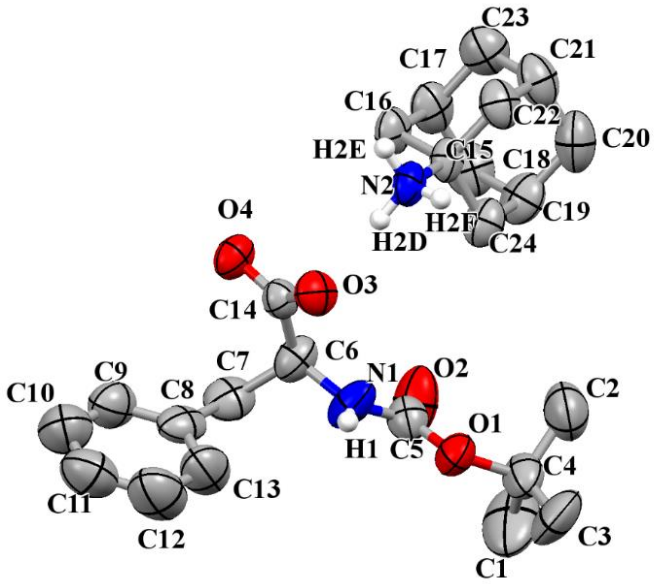

Fig. S11: ORTEP plot of salt **BocF-A** (50% probability)

Table S4: Hydrogen bonding table for salt **BocF-A**

D-H•••A	d(D-A)/Å	d(H•••A)/Å	d(D•••A)/Å	∠D-H•••A/°	Symmetry
N2-H2D•••O3	0.89	1.88	2.774(6)	178	x,y,z
N2-H2E•••O4	0.89	1.88	2.751(6)	164	1-x, -1/2+y,1-z
N2-H2F•••O4	0.89	1.88	2.763(6)	174	x,-1+y, z

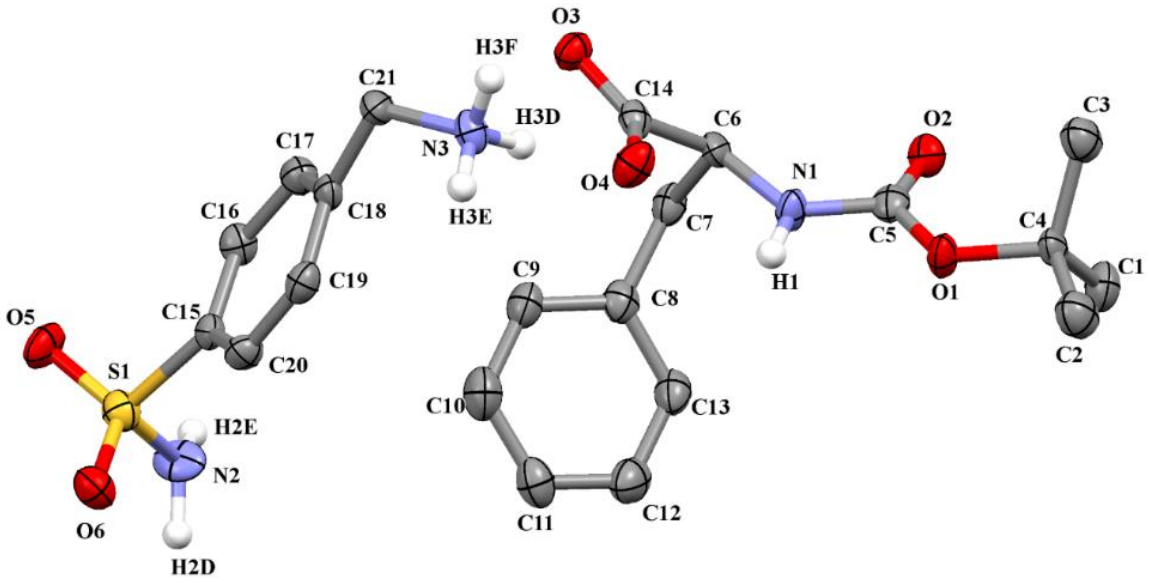

Fig. S12: ORTEP plot of salt **BocF-M** (50% probability)

Table S5: Hydrogen bonding table for salt **BocF-M**

D-H•••A	d(D-A)/Å	d(H•••A)/Å	d(D•••A)/Å	∠D-H•••A/°	Symmetry
N2-H2D•••O2	0.99(7)	1.85(8)	2.825(9)	171	-1+x,-1+y,z
N3-H2D•••O4	0.91	1.82	2.722(8)	170	x,y,z
N3-H2E•••O3	0.91	1.84	2.734(8)	167	x,-1+y, z
N3-H2F•••O3	0.91	2.15	2.947(7)	146	1-x,-1/2+y,1-z

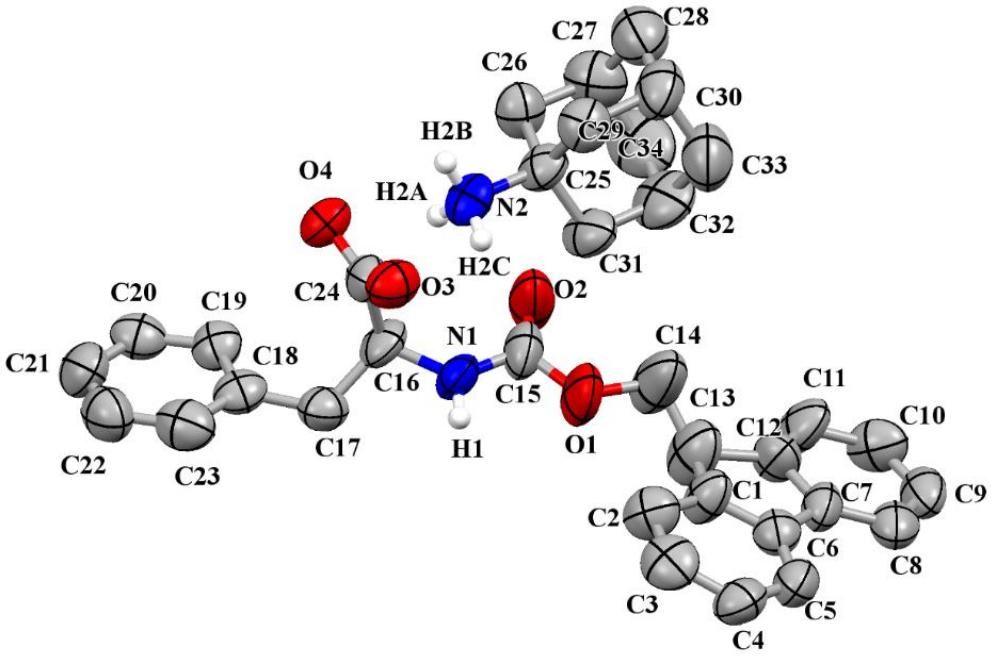

Fig. S13: ORTEP plot of salt **FmocF-A** (50% probability)

Table S6: Hydrogen bonding table for salt **FmocF-A**

D-H•••A	d(D-A)/Å	d(H•••A)/Å	d(D•••A)/Å	∠D-H•••A/°	Symmetry
N2-H2A•••O3	0.91	1.85	2.714(16)	157	x,y,z
N2-H2B•••O4	0.91	2.00	2.808(14)	147	-x, 1/2+y,2-z
N2-H2C•••O4	0.91	1.96	2.805(15)	153	x,1+y, z

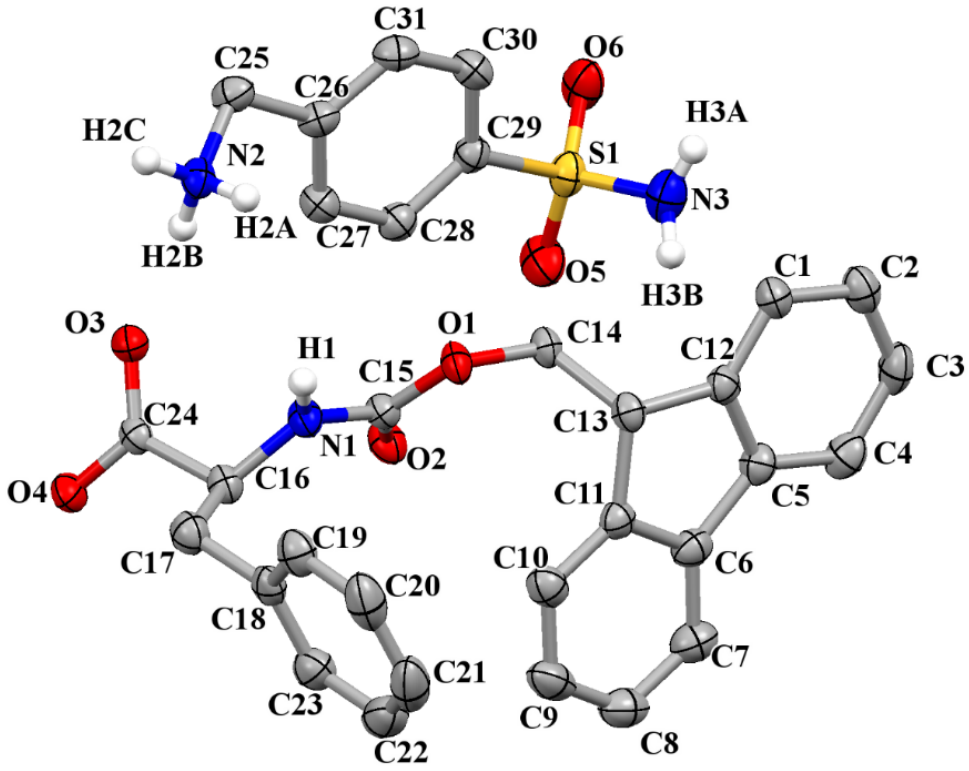

Fig. S14: ORTEP plot of salt **FmocF-M** (50% probability)

Table S7: Hydrogen bonding table for salt **FmocF-M**

D-H•••A	d(D-A)/Å	d(H•••A)/Å	d(D•••A)/Å	∠D-H•••A/°	Symmetry
N1-H1•••O4	0.86	2.07	2.902(5)	164	x,-1+y,z
N2-H2A•••O4	0.89	1.87	2.727(5)	161	x,-1+y,z
N2-H2B•••O3	0.89	1.88	2.737(5)	162	x,-1+y, z
N2-H2C•••O3	0.89	1.96	2.837(5)	170	x,y,z
N3-H3A•••O5	0.79	2.52	3.824(8)	163	1-x, -1/2+y,1-z

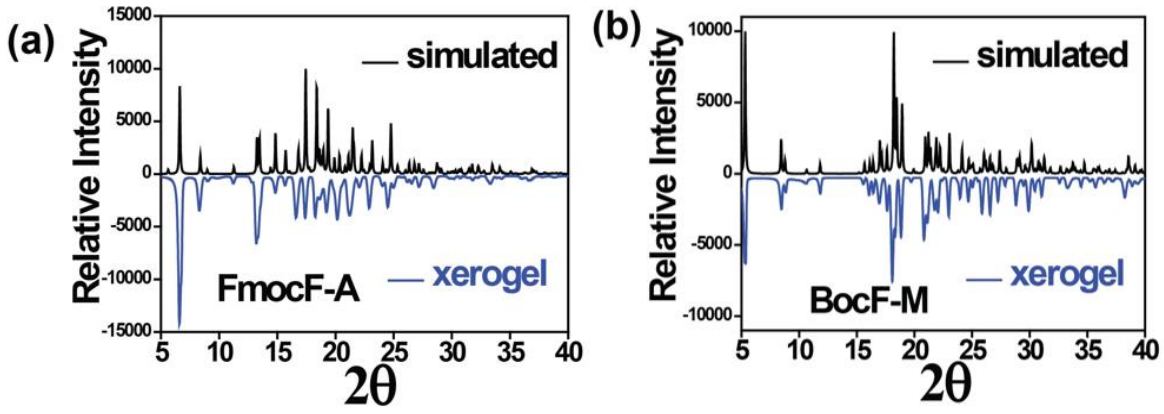

Fig. S15: Powder X-ray diffraction patterns (simulated vs. xerogels) of gelators **(a) FmocF-A**, **(b) BocF-M**

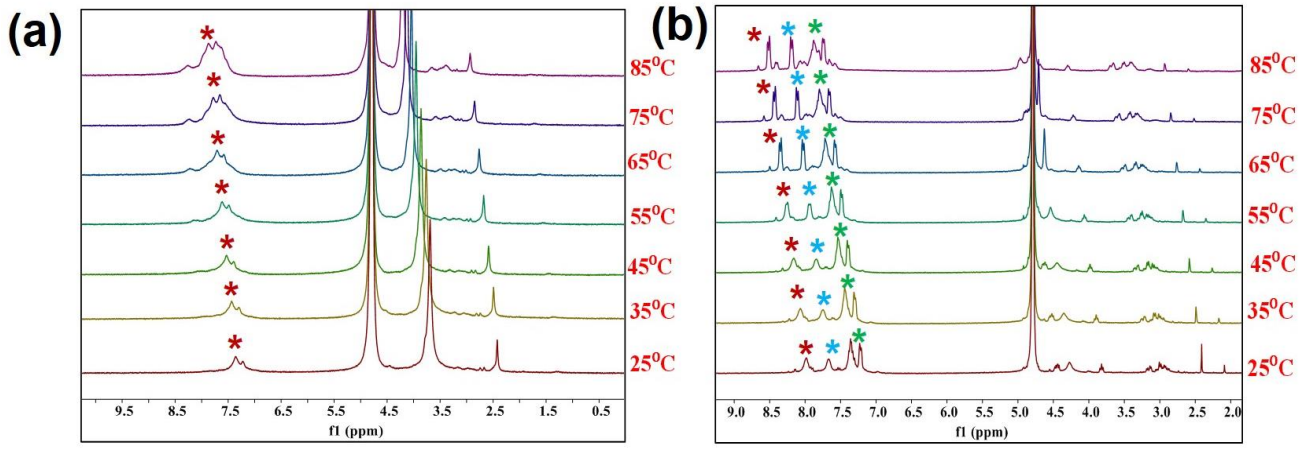

Fig. S16. Temperature –dependent ^{1}H NMR spectra of hydrogels of (a) **FmocFF-T** (at M.G.C 2 wt %) (b) **FmocFF-M** (at M.G.C 1.5 wt %)

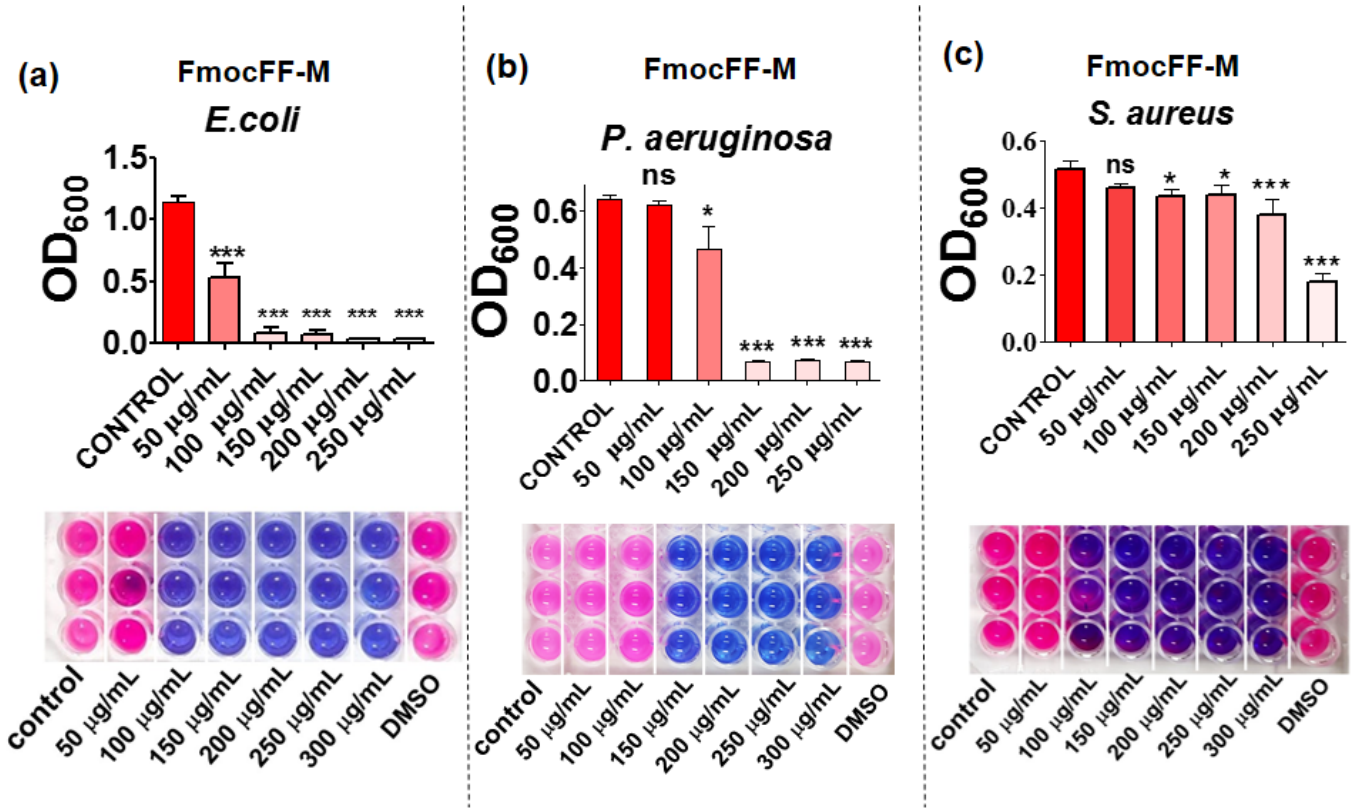

Fig. S17: MIC determination by Turbidity and Resazurin assays of **FmocFF-M** against (a) ***E. coli*** (MIC= **100 µg/mL**) (b) ***P. aeruginosa*** (MIC= **150 µg/mL**) and (c) ***S. aureus*** (MIC=**250 µg/mL**); Data are represented considering mean ± SD where *P < 0.05, **P < 0.01, ***P < 0.001, and ns represents not significant.

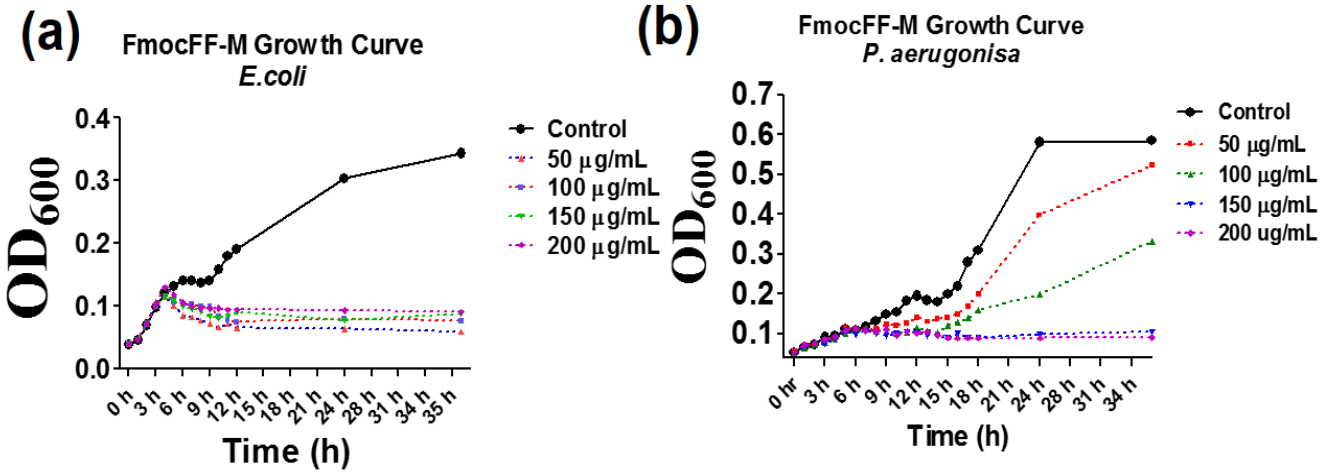

Fig. S18: Bacterial growth curve of **FmocFF-M** against (a) ***E. coli*** (b) ***P. aeruginosa,***

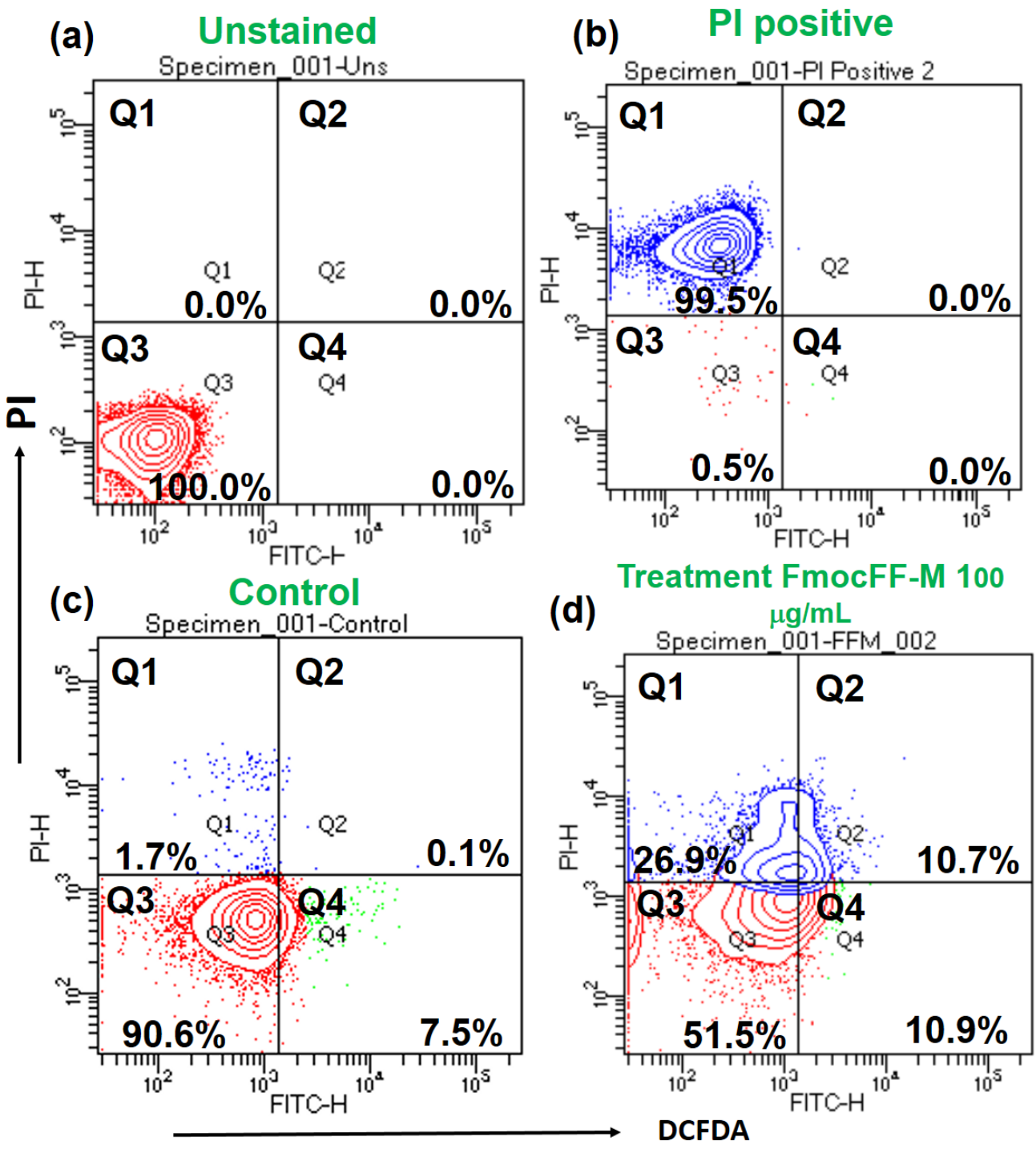

Fig. S19: Flow cytometry of **FmocFF-M** against ***E. coli***; Q3 represents population of healthy cells, Q1 represents the population of PI^+ cells induced by boiling ***E. coli*** cells in water at 100°C, Q4 represents ROS^+ cells and Q2 represents both PI^+ and ROS^+ cells; (a) unstained (b) only PI^+ stained cells after boiling ***E. coli*** cells in water at 100°C (c) and (d) control and treated ***E. coli*** cells respectively stained with both PI and DCFDA

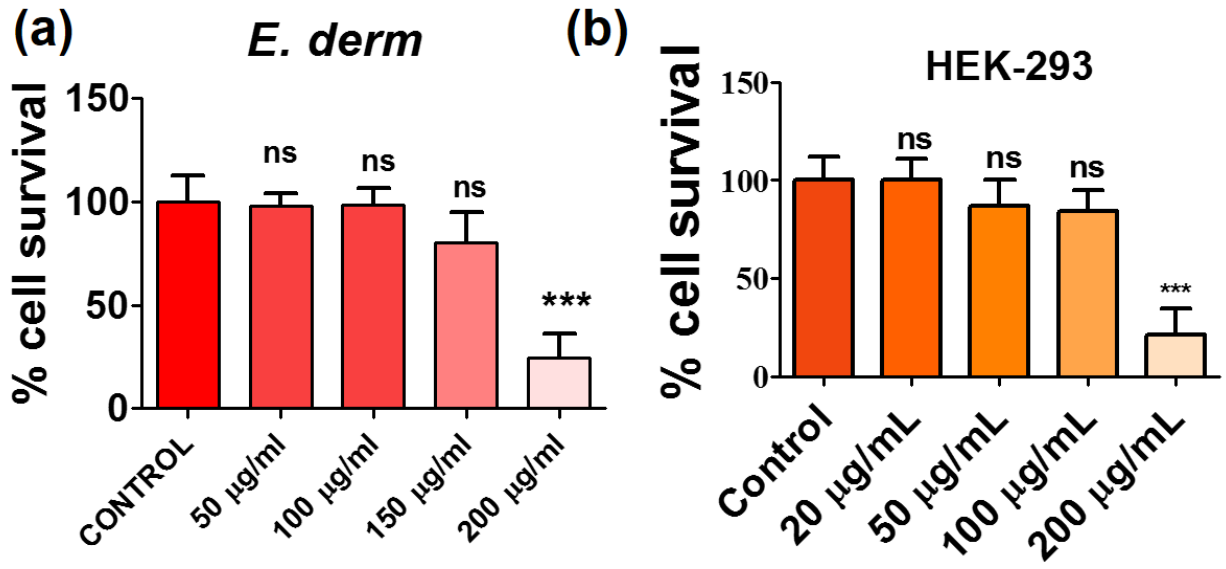

Fig. S20: Cytotoxicity evaluation of **FmocFF-M** by MTT assay against (a) ***E.derm*** (b) **HEK 293;** Data are represented considering mean ± SD where *P < 0.05, **P < 0.01, ***P < 0.001, and ns represents not significant.

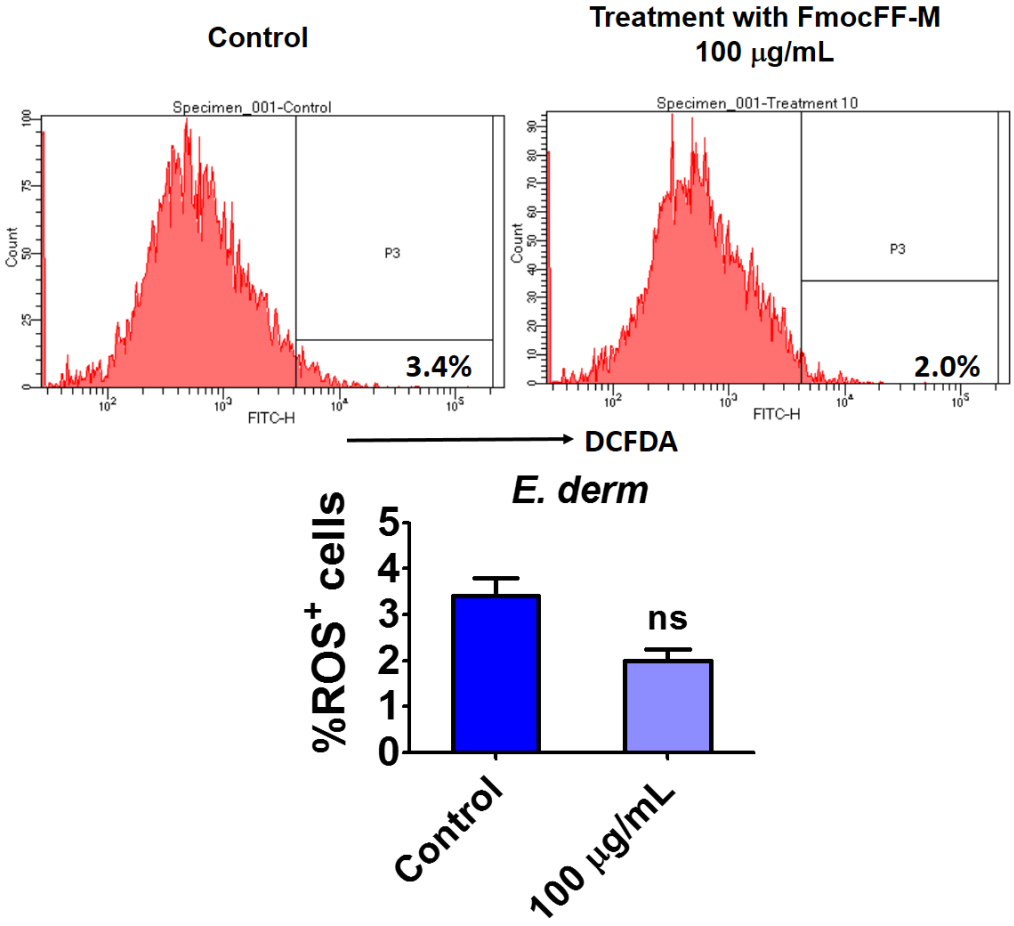

Fig. S21: DCFDA (dichlorodihydrofluoroscein diacetate) assay shown by **FmocFF-M** against ***E. derm*** (treatment: 100 µg/mL, 2 h)

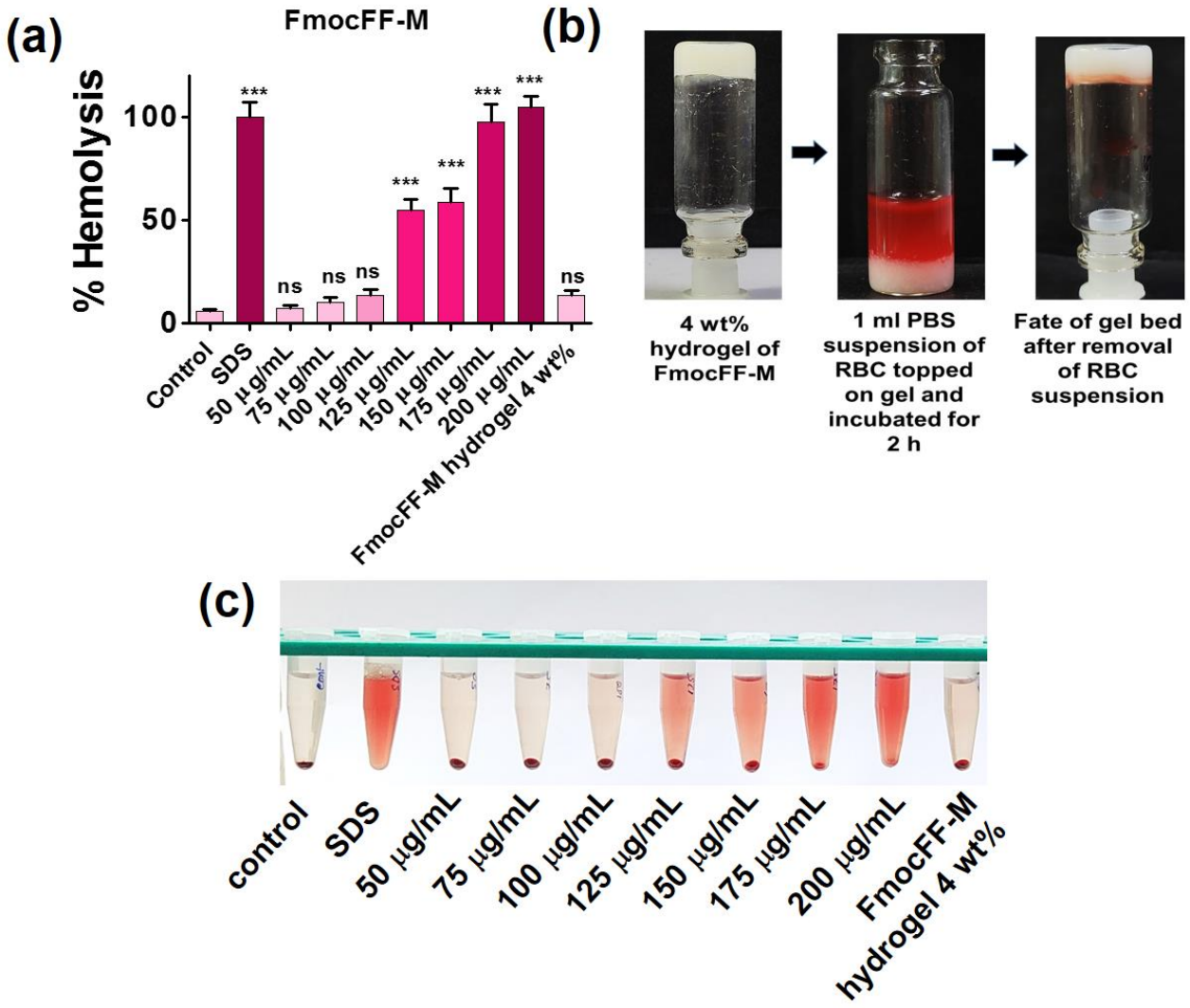

Fig. S22: Hemolysis: (a) % hemolysis by **FmocFF-M** and **FmocFF-M** hydrogel, (b) hemolysis experiment perform on **FmocFF-M** hydrogel bed and (c) visual observation of hemolysis; nearly negligible %hemolysis with 4 wt % FmocFF-M hydrogel in comparison with 100% hemolysis with much less amount of FmocFF-M (200 μg/mL) was due to slow and sustained release of the active component from the hydrogel thereby making the topical hydrogel safe for application. Data are represented considering mean ± SD where *P < 0.05, **P < 0.01, ***P < 0.001, and ns represents not significant

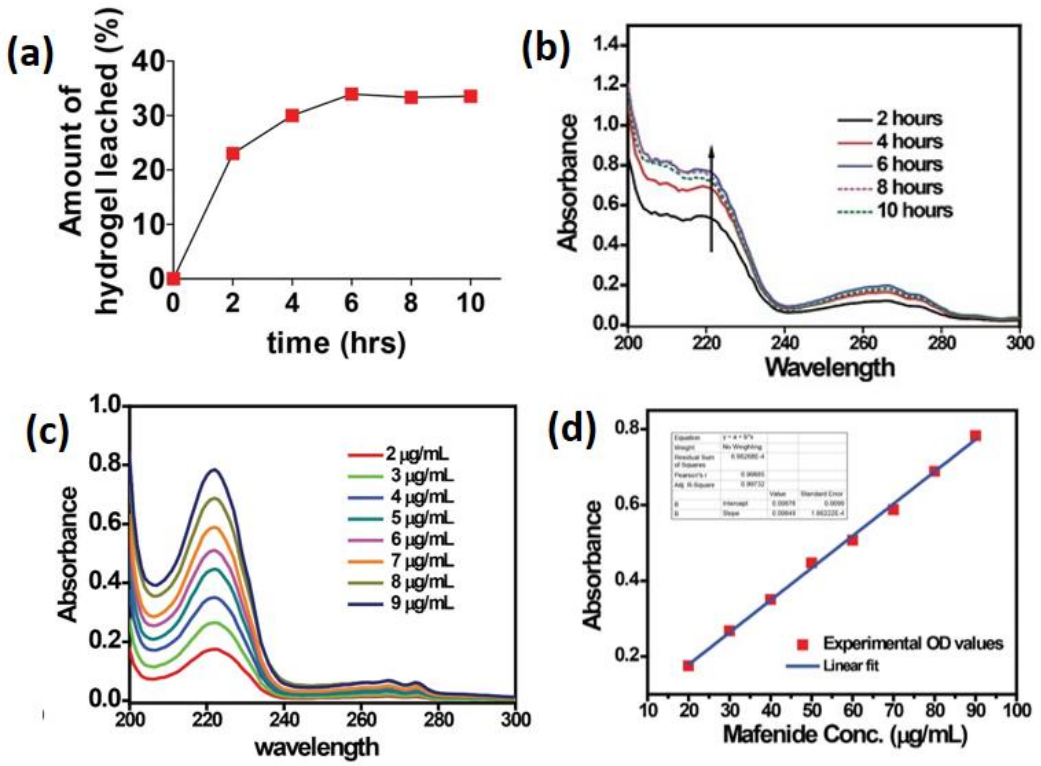

Fig. S23: **(a)** Mafenide release from the **FmocFF-M** hydrogel-bed (4 wt %) **(b)** UV-vis spectra of distilled water aliquots from drug-release experiment; **(c)** UV-vis absorption spectra of Mafenide in water; **(d)** Calibration curve of Mafenide with Linear Fit.

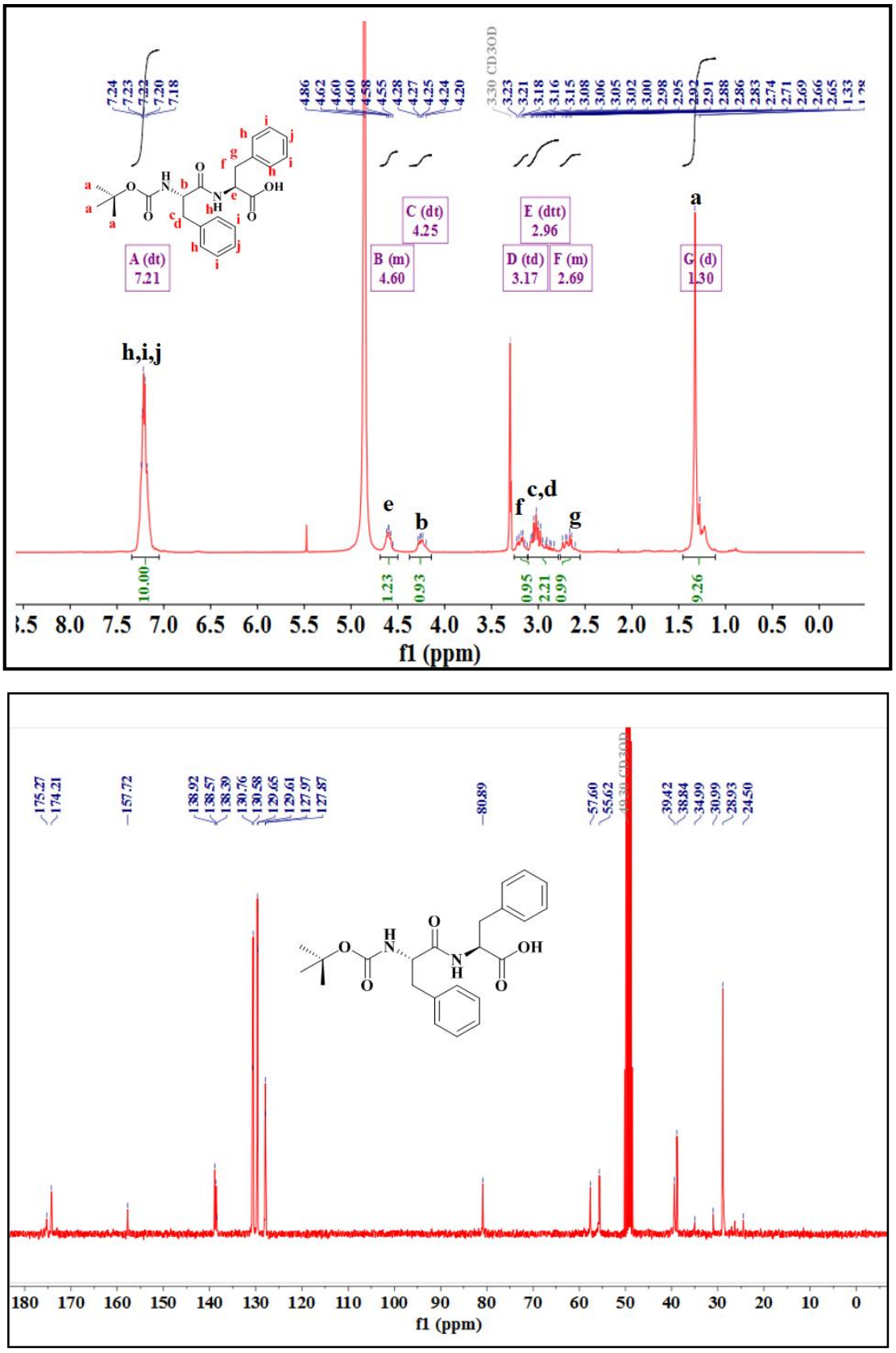

Fig. S24: ^{1}HNMR and ^{13}CNMR of **BocFF** in CD_3OD.

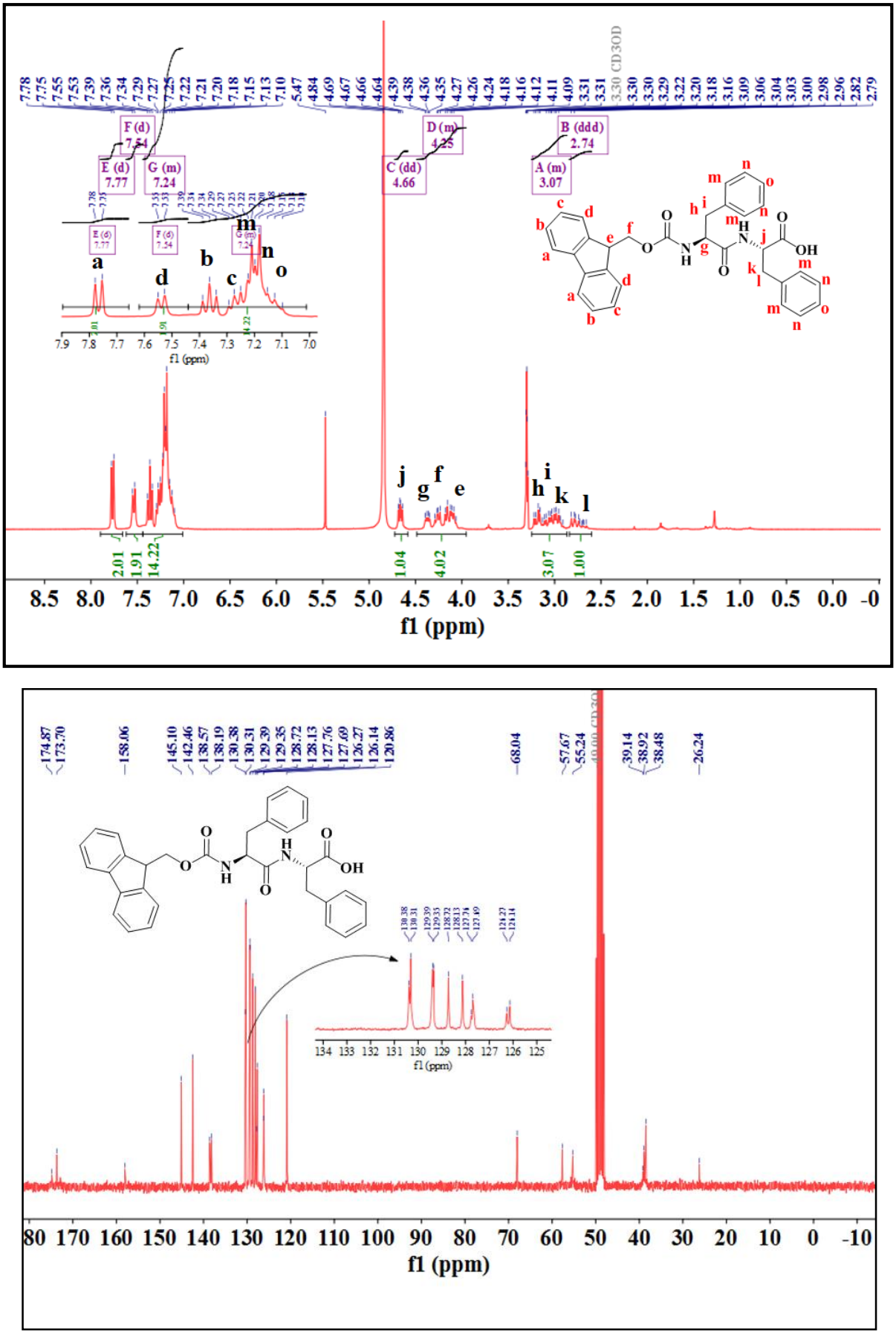

Fig. S25: ^{1}HNMR and ^{13}CNMR of **FmocFF** in CD_3OD.

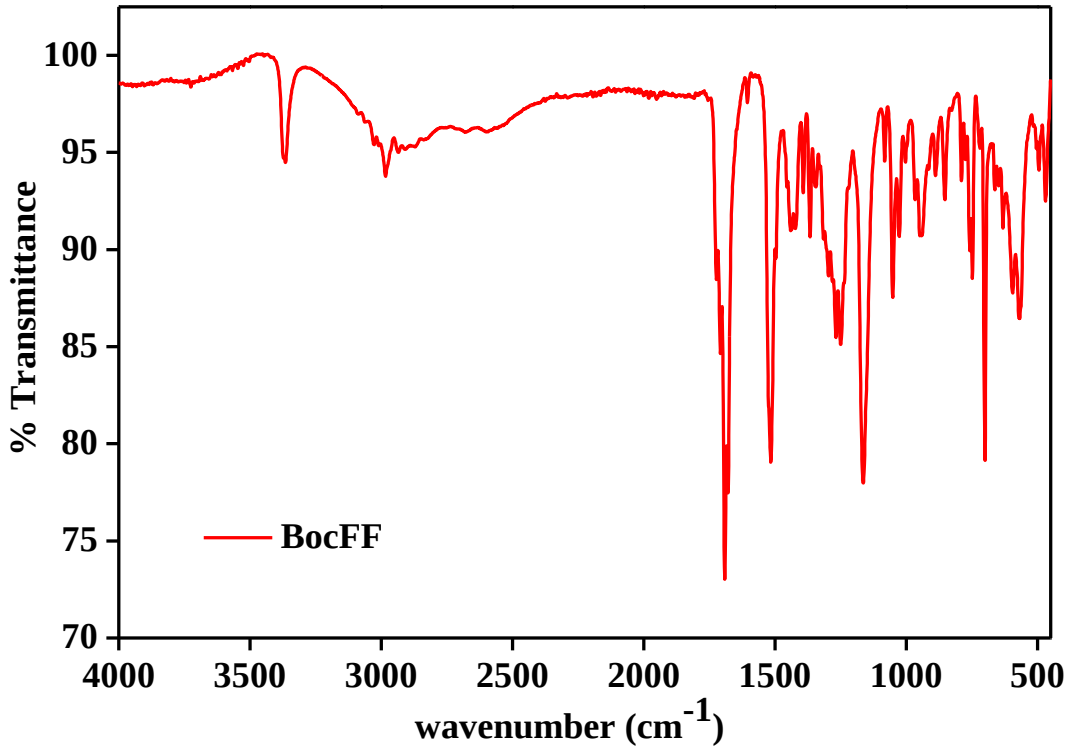

Fig. S26: FT-IR spectra of **BocFF.**

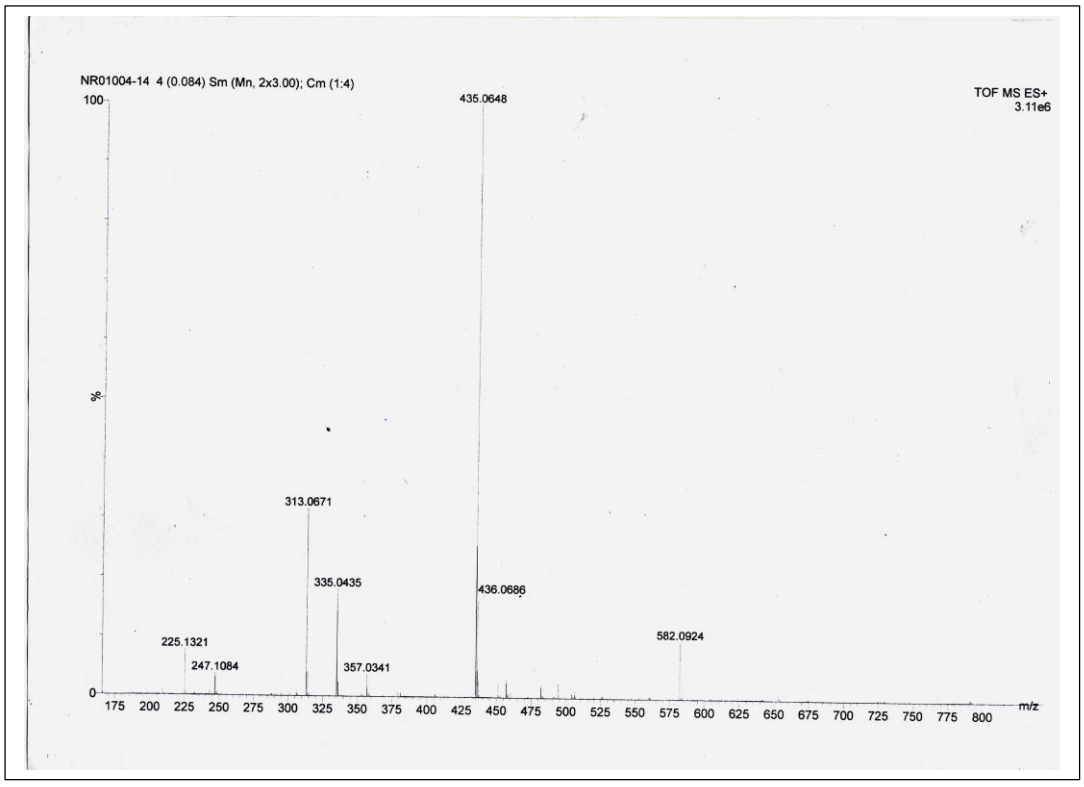

Fig. S27: ESI HR-MASS of **BocFF** obtained at **$[M+Na]^+$= 435.0648** ***m/z***

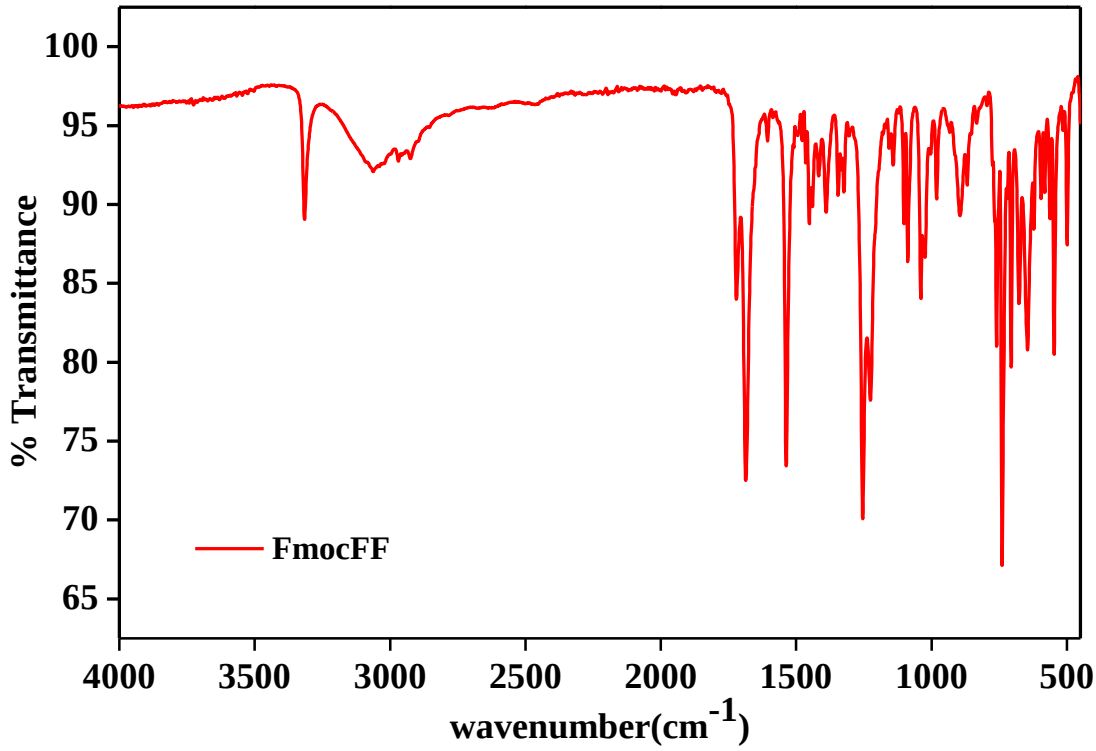

Fig. S28: FT-IR spectra of **FmocFF.**

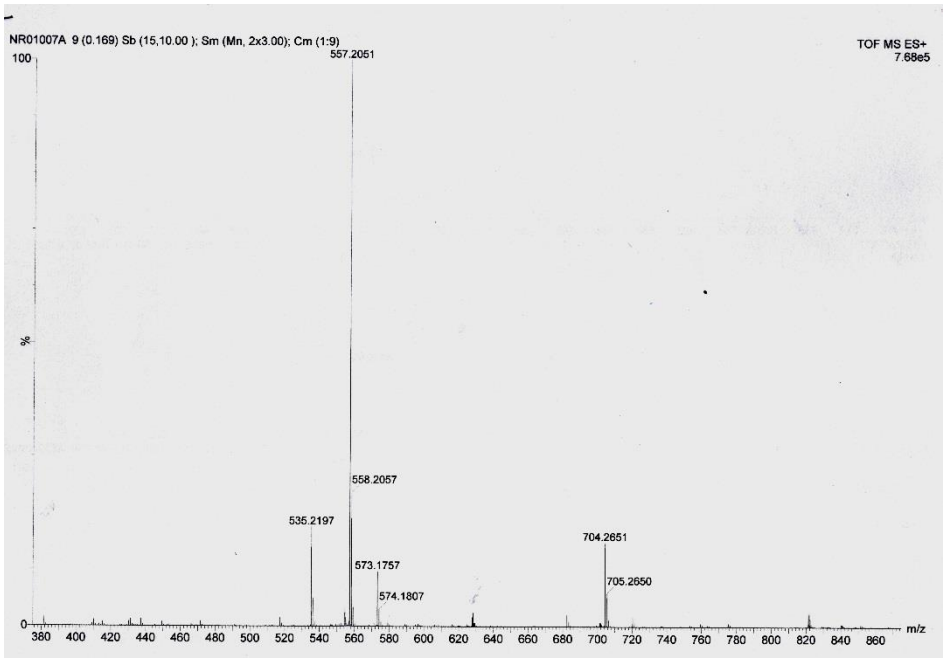

Fig. S29: ESI HR-MASS of **FmocFF** obtained at **$[M+Na]^+$= 557.2051 *m/z***

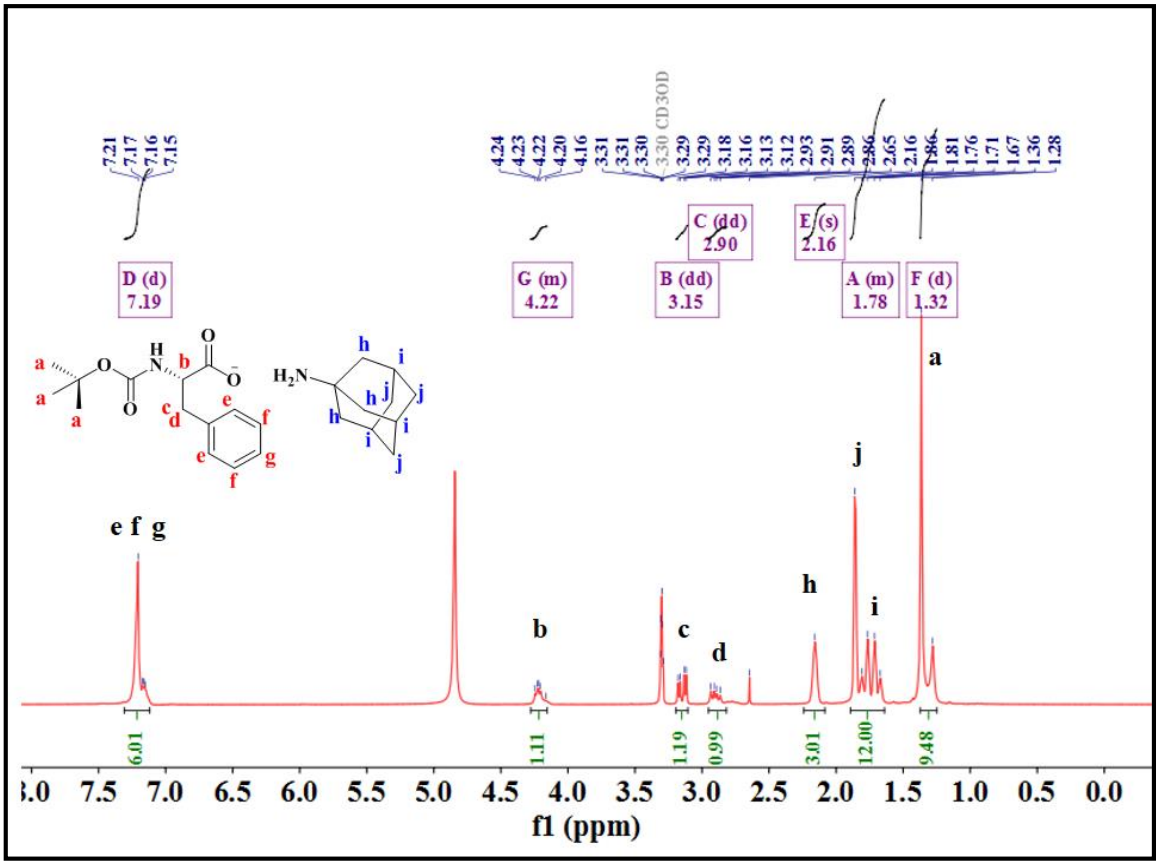

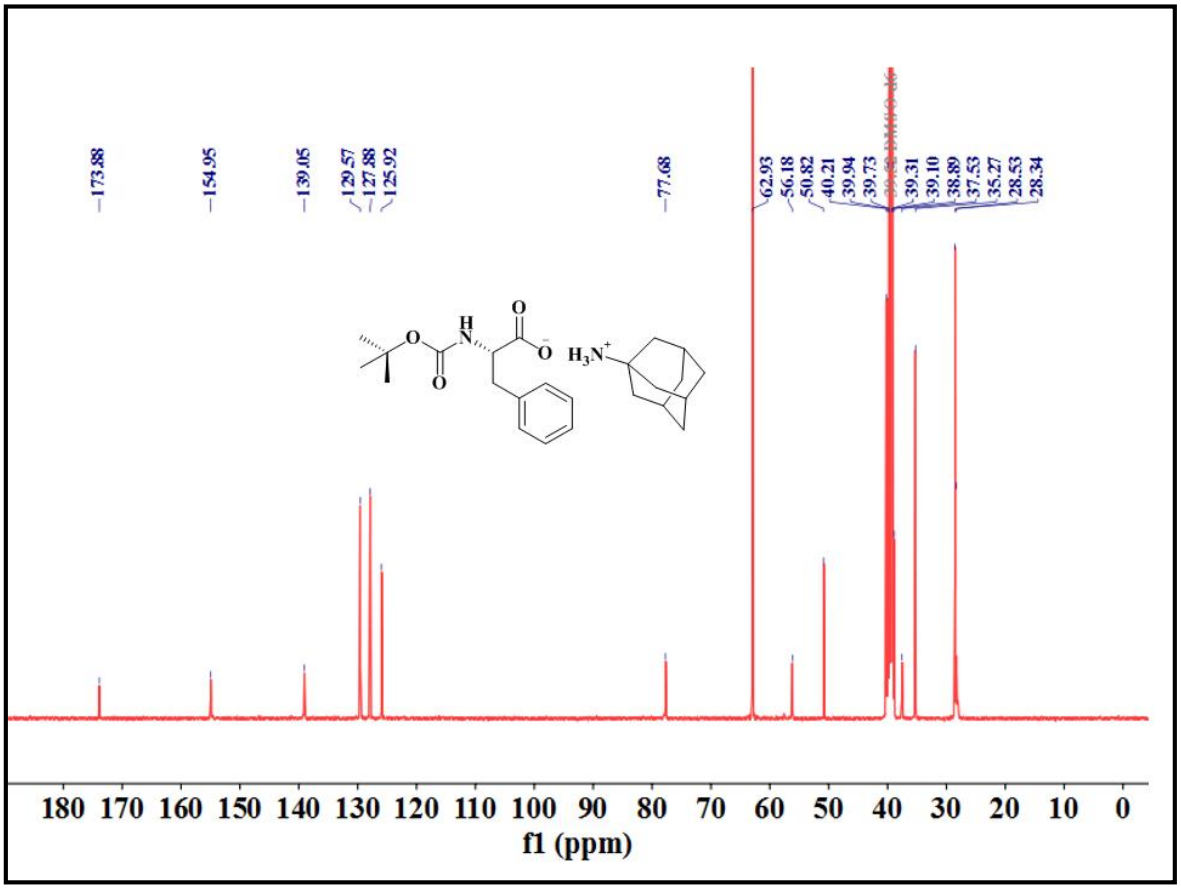

Fig. S30: ^{1}HNMR and ^{13}CNMR of **BocF-A**

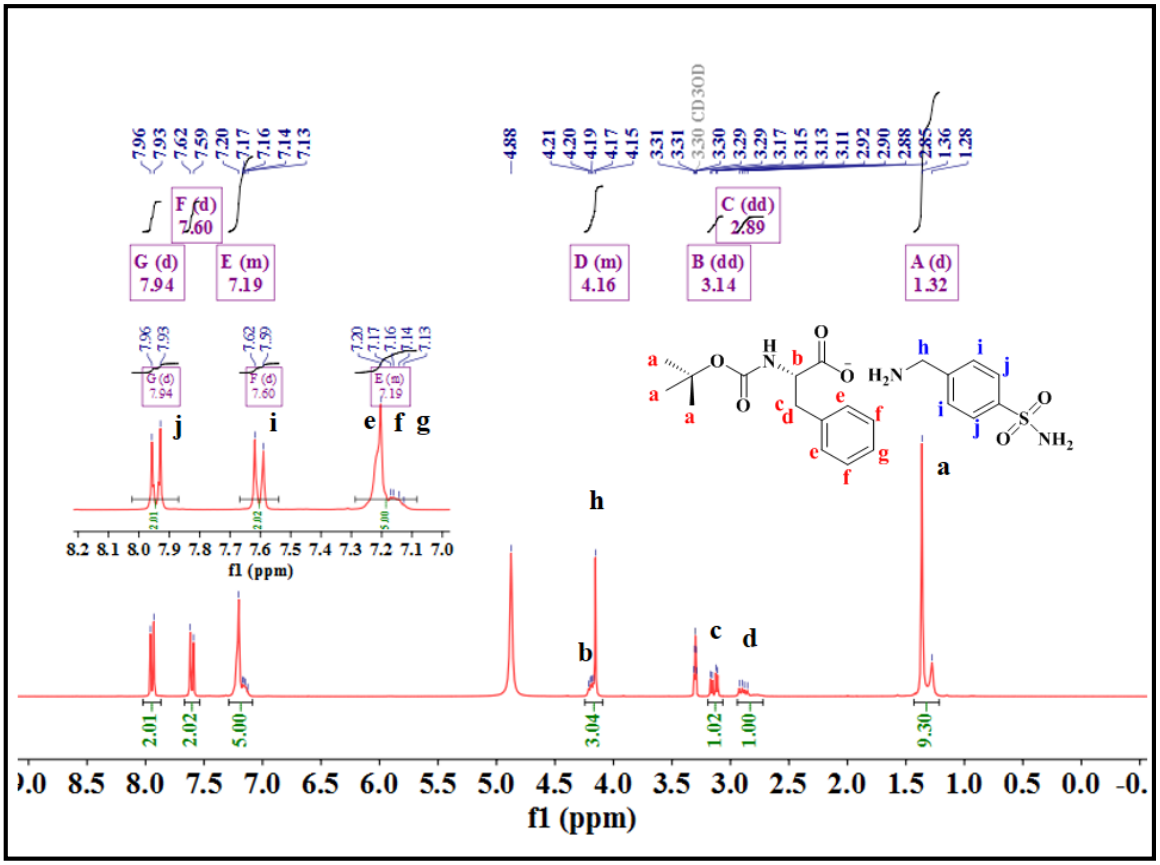

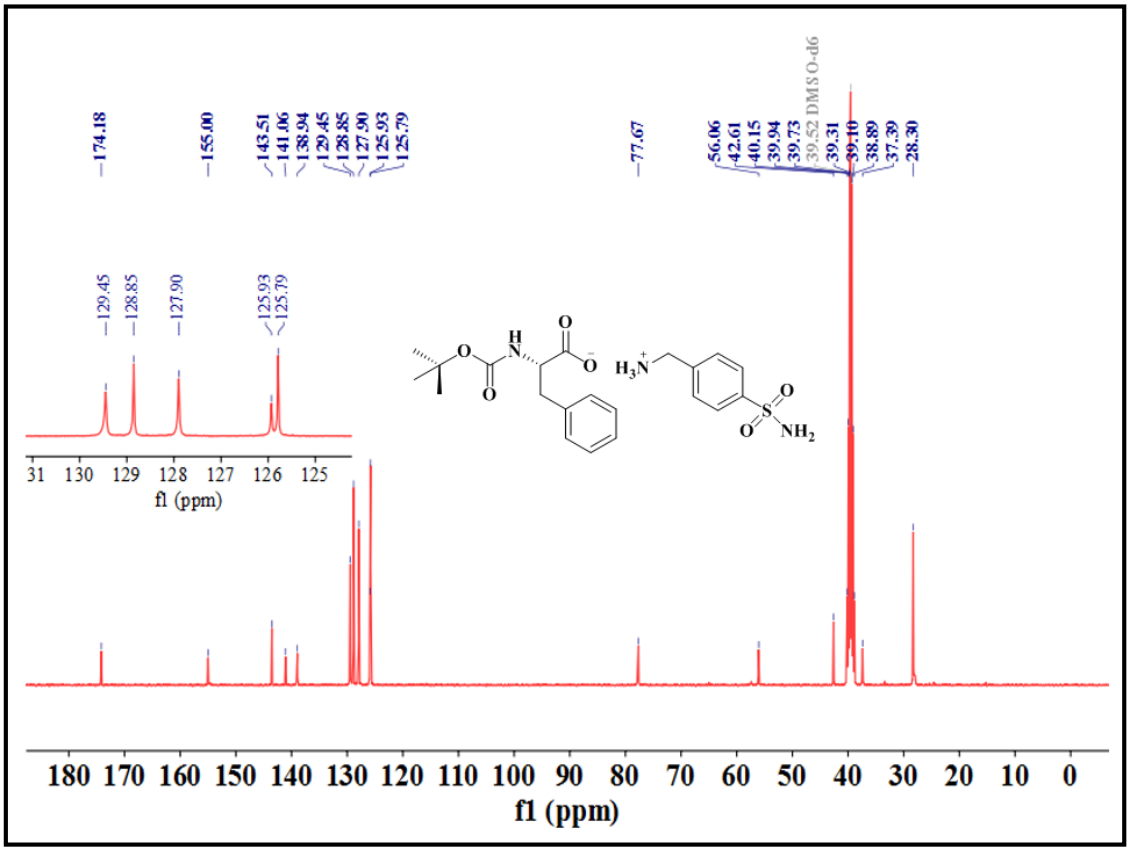

Fig. S31: ^{1}HNMR and ^{13}CNMR of **BocF-M**

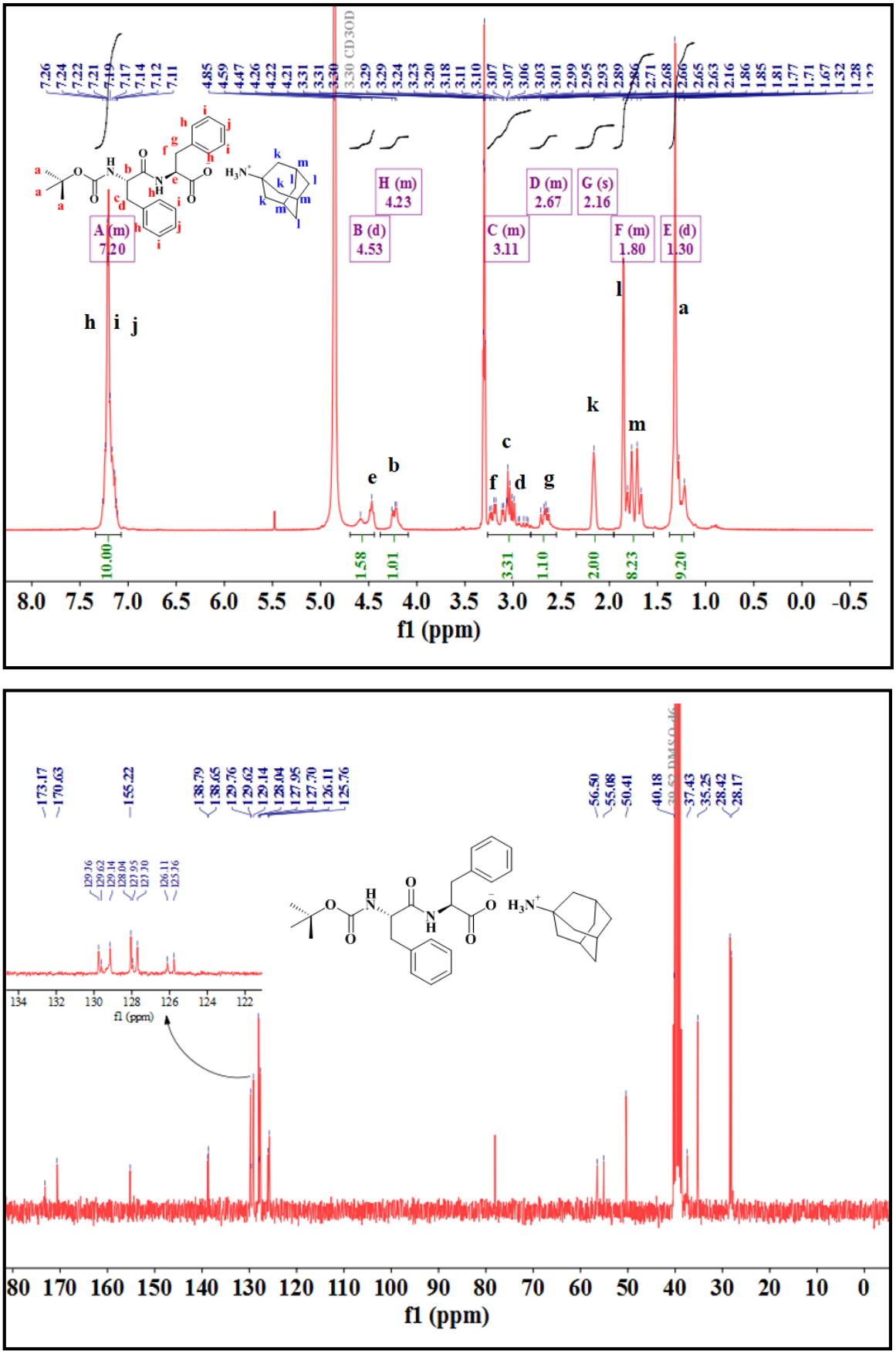

Fig. S32: ^{1}HNMR and ^{13}CNMR of **BocFF-A**

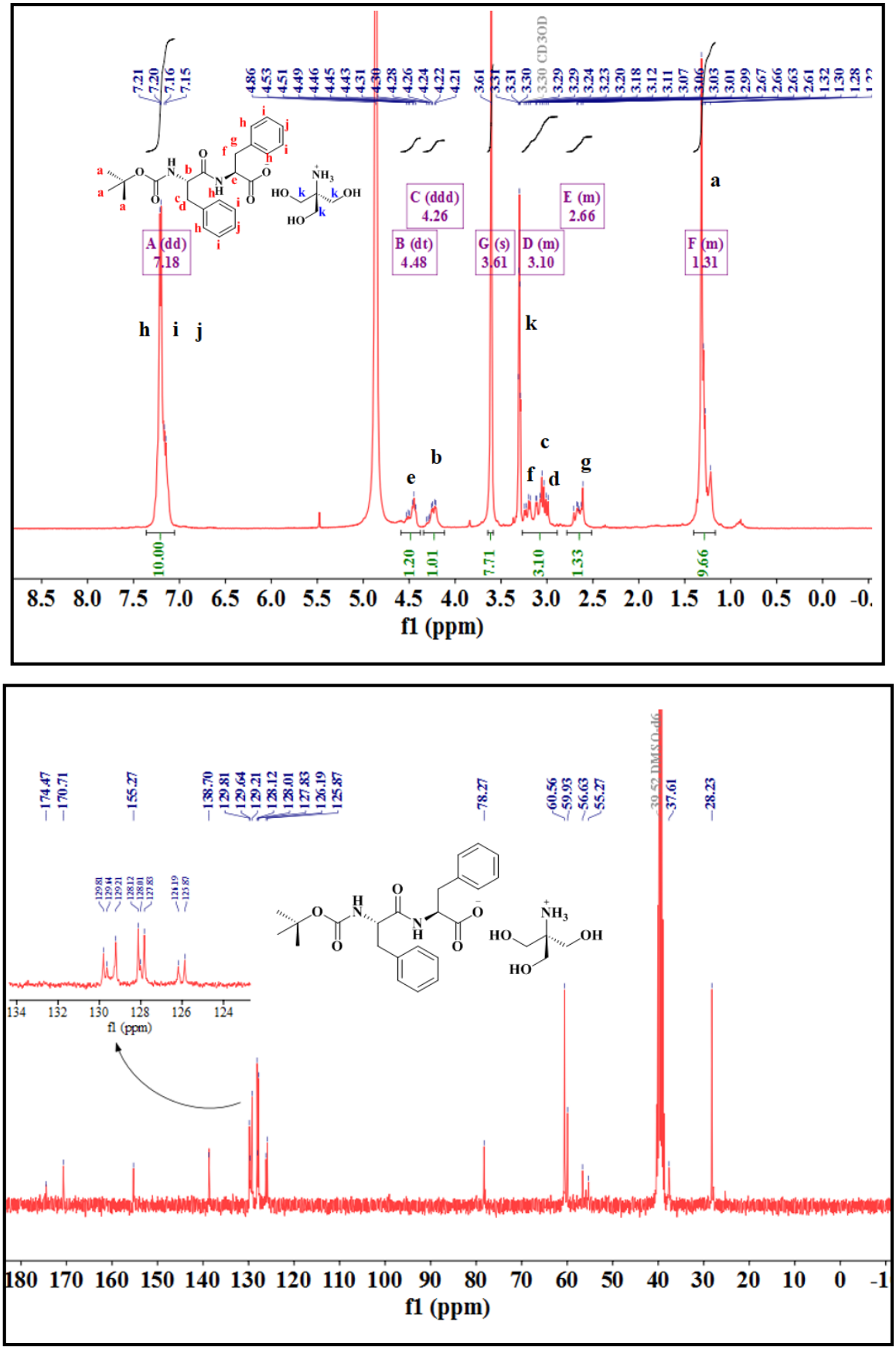

Fig. S33: ^{1}HNMR and ^{13}CNMR of **BocFF-T**

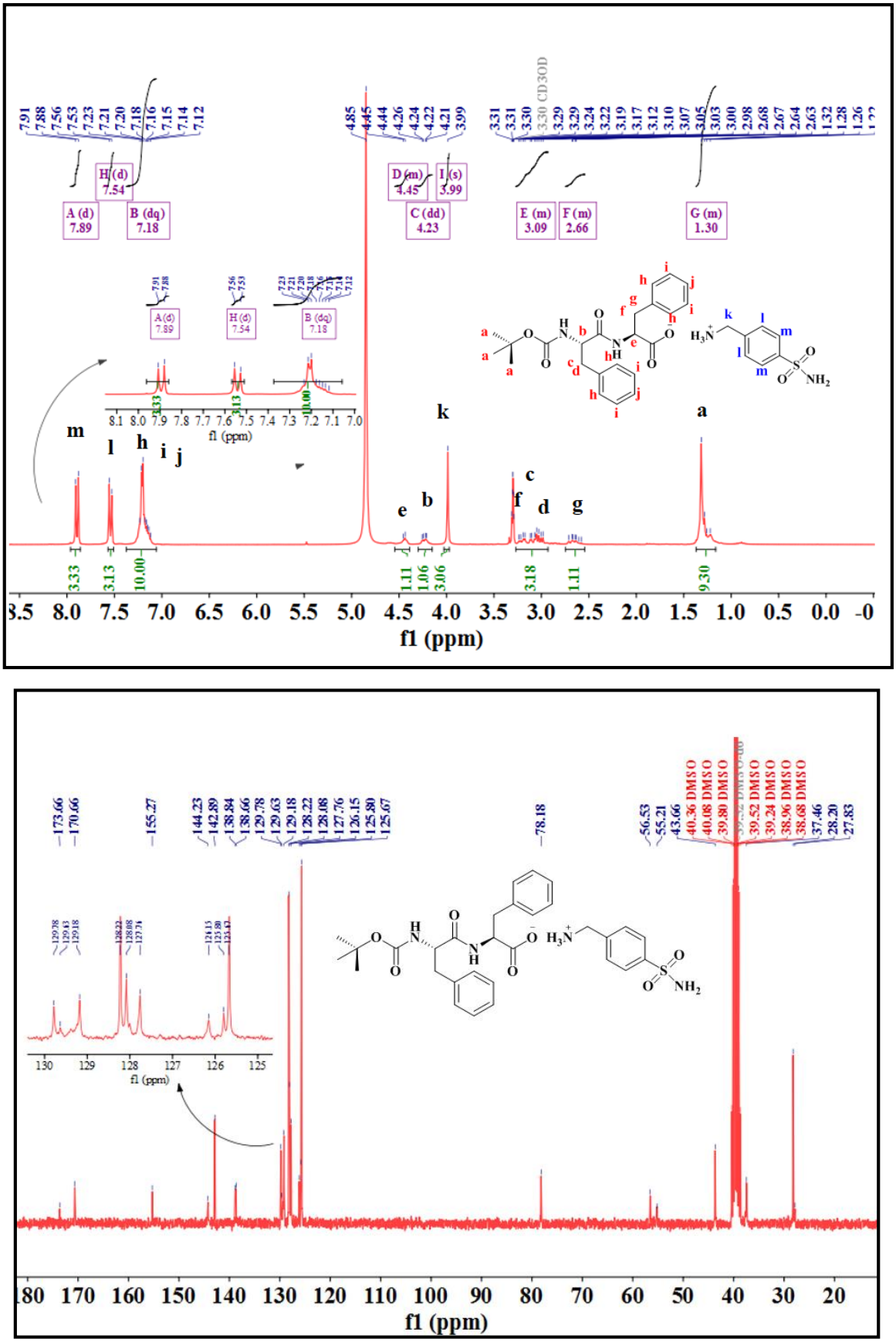

Fig. S34: ^{1}HNMR and ^{13}CNMR of **BocFF-M**

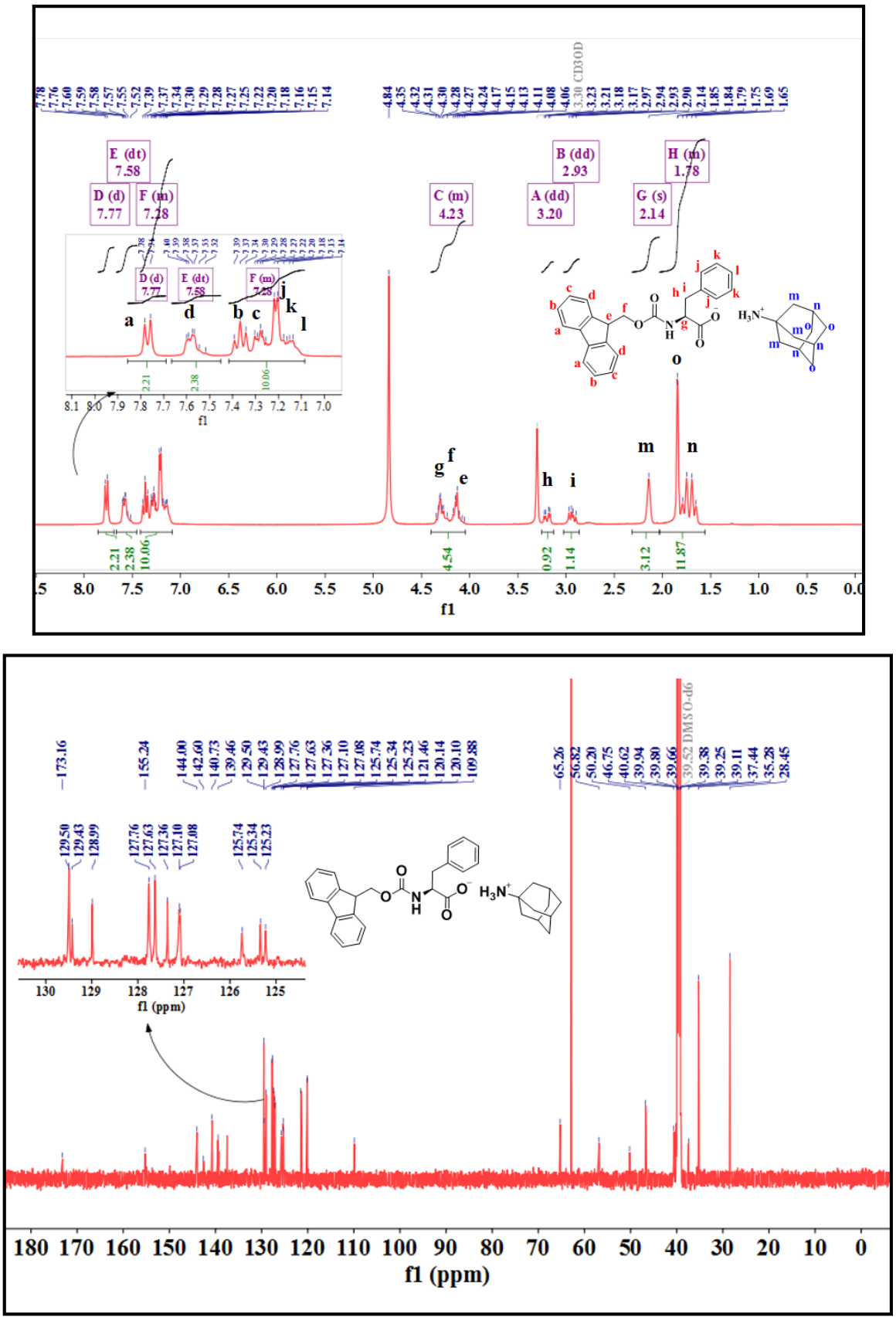

Fig. S35: ^{1}HNMR and ^{13}CNMR of **FmocF-A**

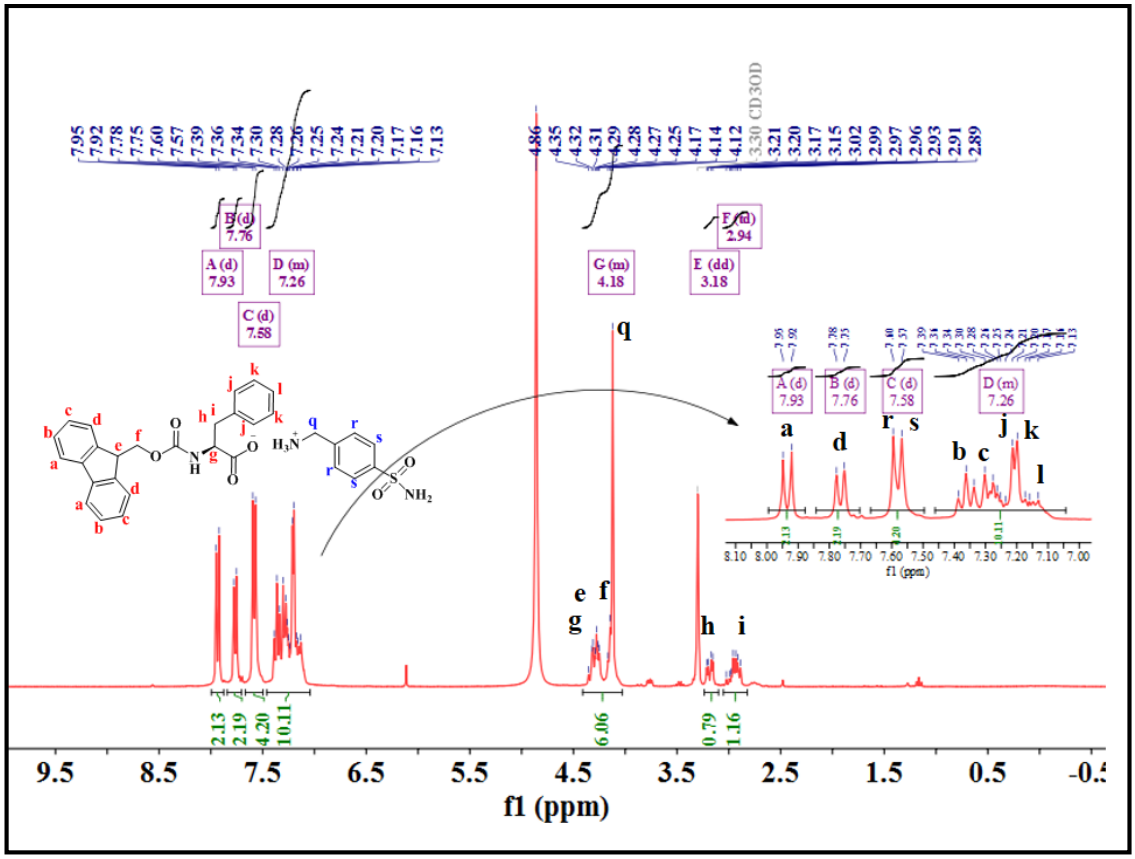

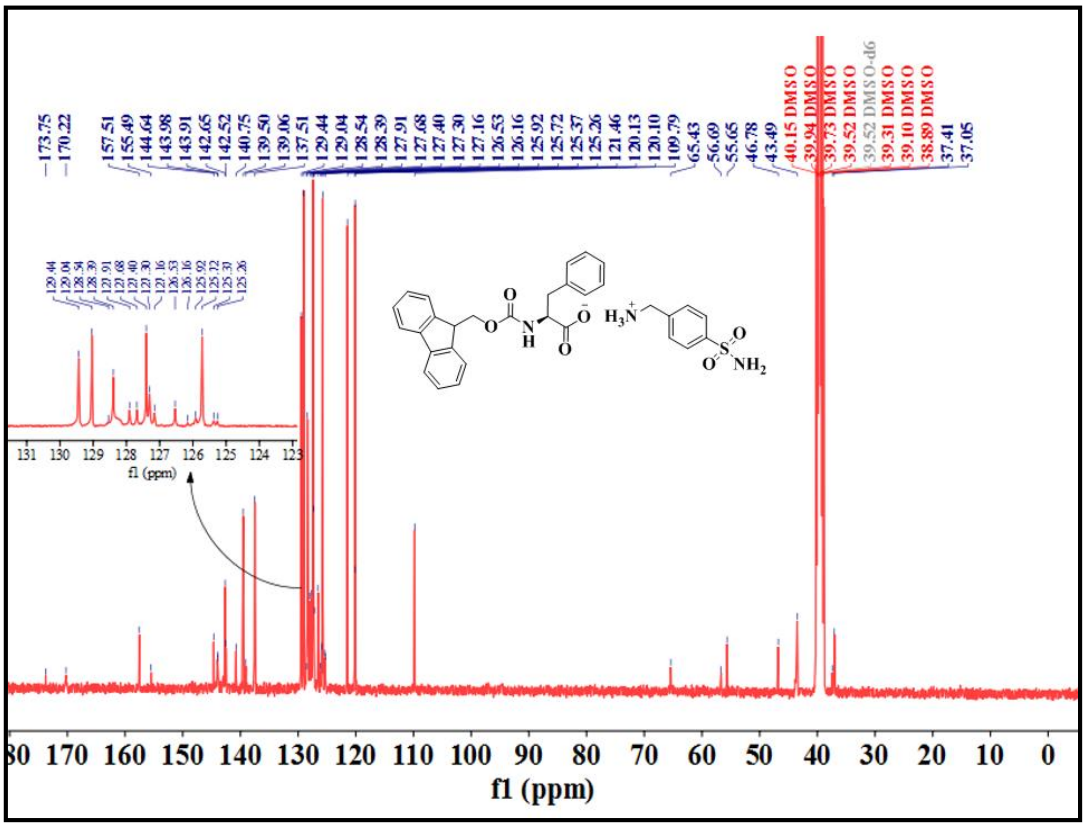

Fig. S36: ^{1}HNMR and ^{13}CNMR of **FmocF-M**

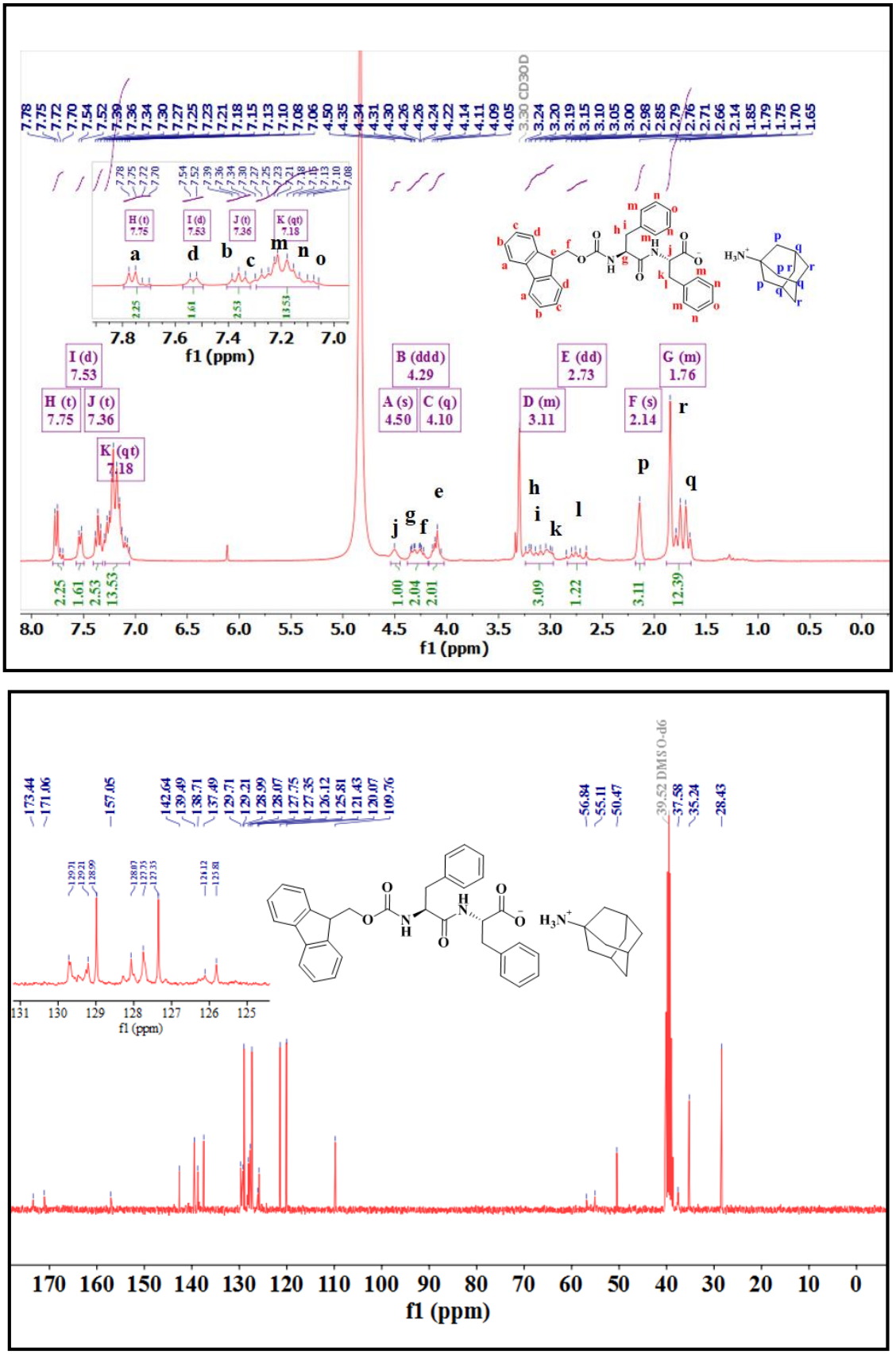

Fig. S37: ^{1}HNMR and ^{13}CNMR of **FmocFF-A**

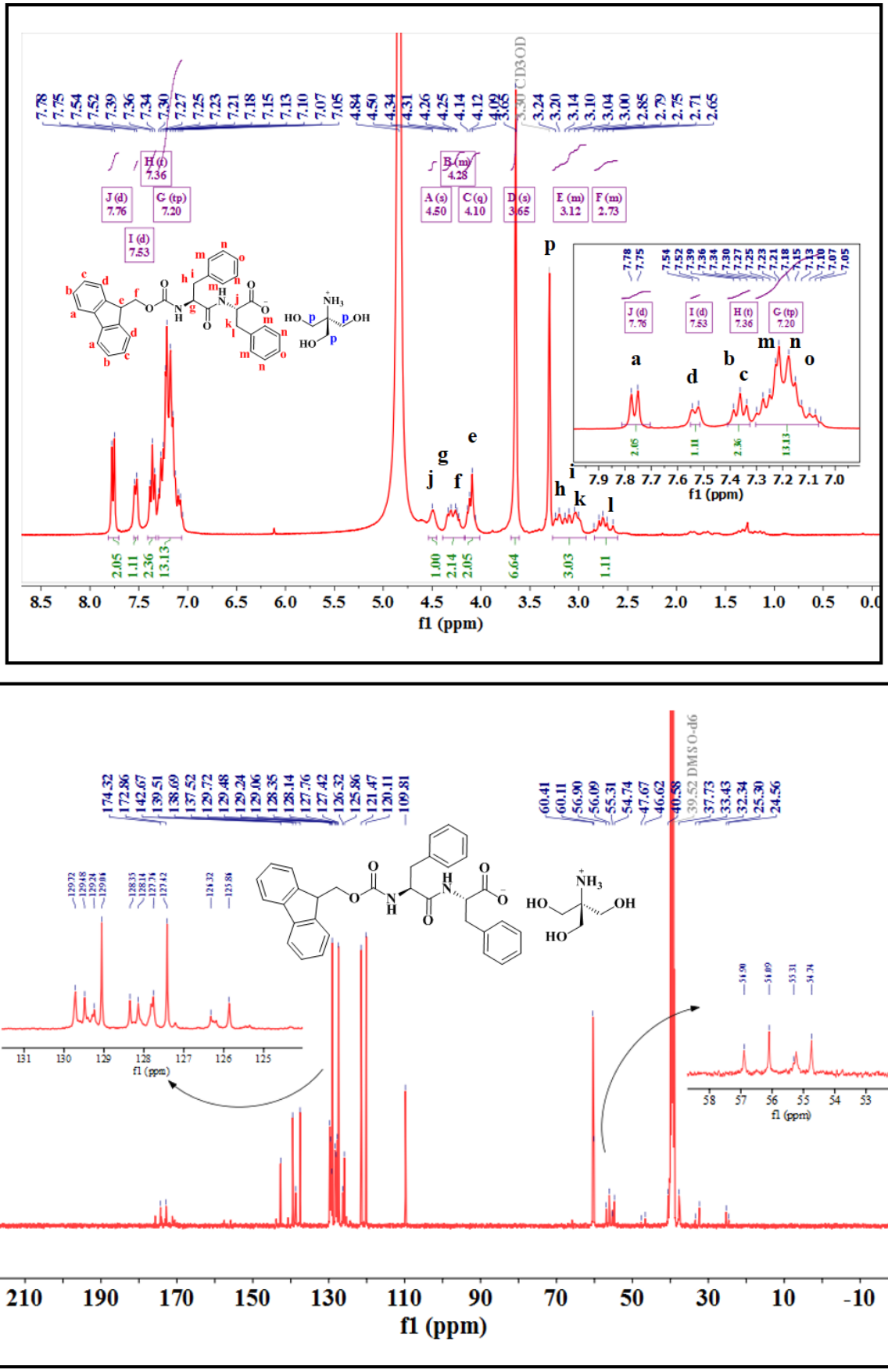

Fig. S38: ^{1}HNMR and ^{13}CNMR of **FmocFF-T**

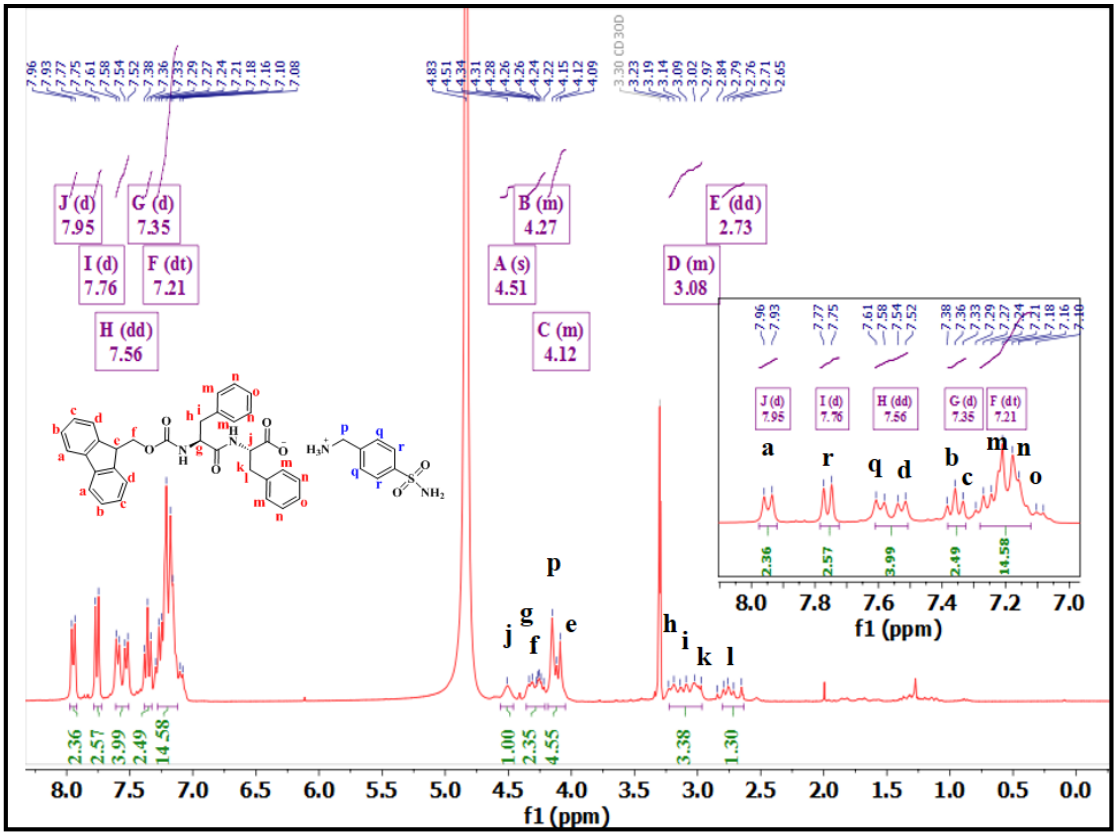

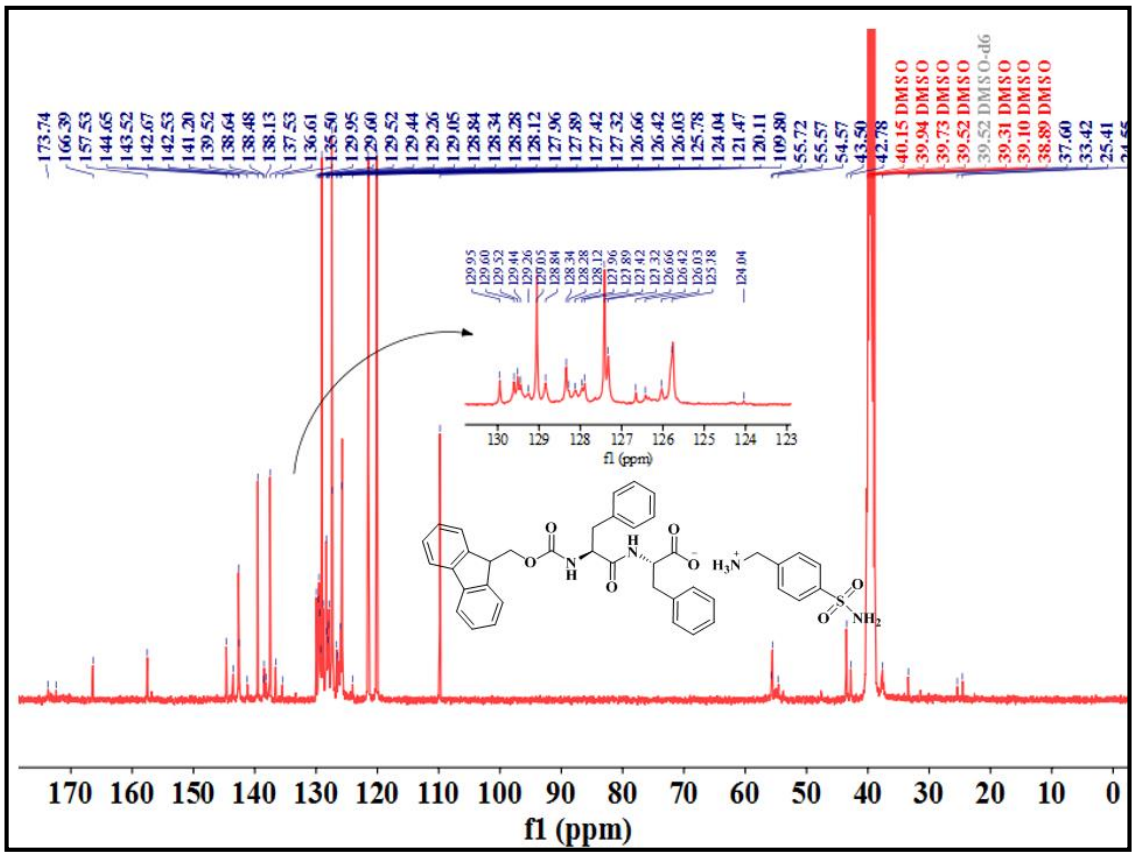

Fig. S39: ^{1}HNMR and ^{13}CNMR of **FmocFF-M**

Table S8: Approximate shifts in the **>C=O** stretching frequencies (in free acids and salts) due to salt formation:

ORGANIC SALTS	COMPONENT ACIDS	>C=O$_{-COOH}$ stretching frequencies in ACIDS (ν_1 cm^{-1})	>C=O$_{-COO^-}$ stretching frequencies in SALTS (ν_2 cm^{-1})	$\Delta\nu$ cm^{-1} = (ν_1-ν_2) cm^{-1}
BocF-A	BocF	1726	1671	55
BocF-M	BocF	1726	1700	26
BocFF-A	BocFF	1722	1705	17
BocFF-T	BocFF	1722	1681	41
BocFF-M	BocFF	1722	1693	29
FmocF-A	FmocF	1720	1725	-5*
FmocF-M	FmocF	1720	1716	4*
FmocFF-A	FmocFF	1710	1695	15
FmocFF-T	FmocFF	1710	1693	17
FmocFF-M	FmocFF	1710	1693	17

* FTIR data clearly did not indicate a considerable shift in stretching frequencies .However, from other characterisation data (single-crystal XRD) salt formation was confirmed (Fig. S13-S14)

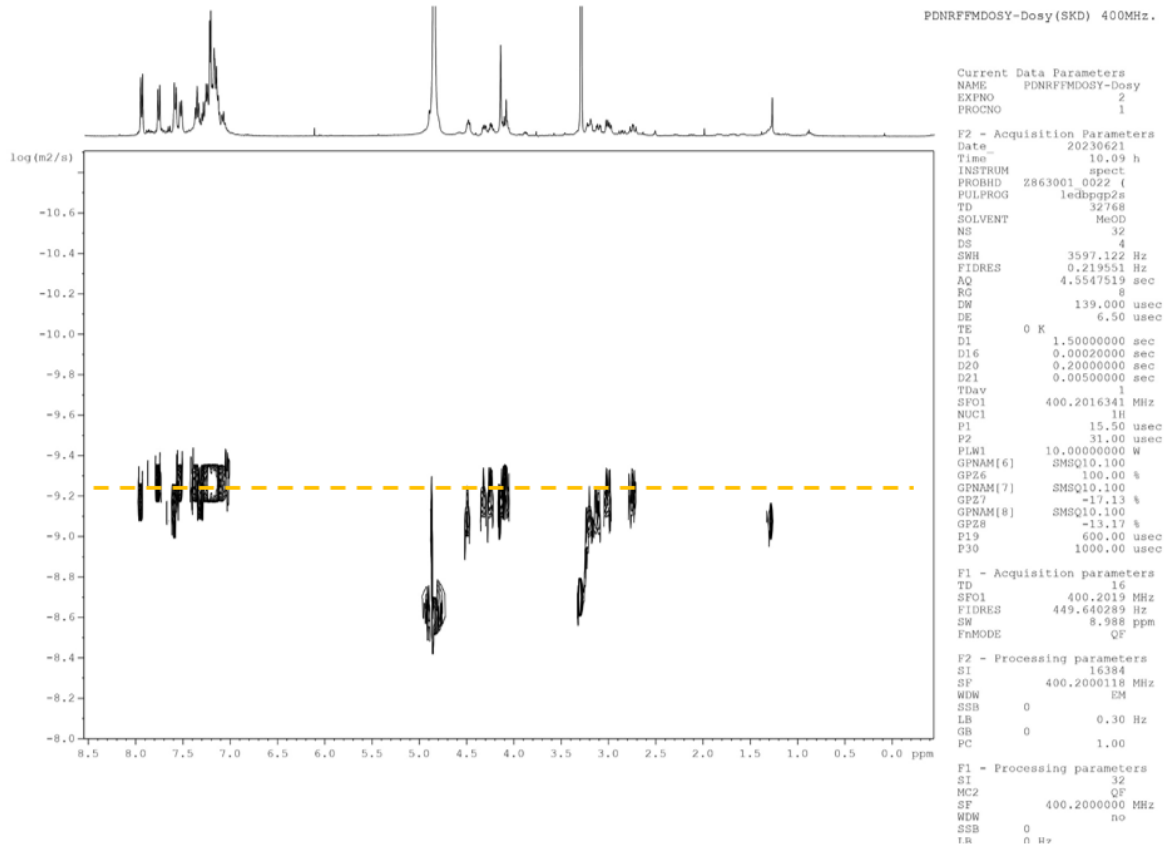

Fig. S40: DOSY NMR of **FmocFF-M** (10 mg in 600 μl of MeOD, 400 MHz). All the protons were located on the same horizontal line suggesting the existence of **FmocFF-M** as a single entity (salt) in solution. This data clearly established the purity of the lead compound **FmocFF-M.**